



Published in final edited form as:

*Chem Soc Rev.* 2012 April 7; 41(7): 2943–2970. doi:10.1039/c2cs15355f.

## Intrinsic Therapeutic Applications of Noble Metal Nanoparticles: Past, Present and Future\*\*

Rochelle R. Arvizo<sup>1</sup>, Sanjib Bhattacharyya, Rachel Kudgus, Karuna Giri<sup>1</sup>, Resham Bhattacharya<sup>1</sup>, and Priyabrata Mukherjee<sup>1,2,3,\*</sup>

<sup>1</sup>Department of Biochemistry and Molecular Biology, Mayo Clinic College of Medicine, Rochester, MN 55905

<sup>2</sup>Department of Physiology and Biomedical Engineering, Mayo Clinic College of Medicine, Rochester, MN 55905

<sup>3</sup>Mayo Clinic Cancer Center, Mayo Clinic College of Medicine, Rochester, MN 55905

### Overview

Biomedical nanotechnology is an evolving field having enormous potential to positively impact the health care system. Important biomedical applications of nanotechnology that may have potential clinical applications include targeted drug delivery, detection/diagnosis and imaging. Basic understanding of how nanomaterials, the building blocks of nanotechnology, interact with the cells and their biological consequences are beginning to evolve. Noble metal nanoparticles such as gold, silver and platinum are particularly interesting due to their size and shape dependent unique optoelectronic properties. These noble metal nanoparticles, particularly of gold, have elicited lots of interest for important biomedical applications because of their ease of synthesis, characterization and surface functionalization. Furthermore, recent investigations are demonstrating another promising applications of these nanomaterials as self-therapeutics. To realize the potential promise of these unique inorganic nanomaterials for future clinical translation, it is of utmost importance to understand few critical parameters; (i) how these nanomaterials interact with the cells at the molecular level; (ii) how their biodistribution and pharmacokinetics influenced by their surface and routes of administration; (iii) mechanism of their detoxification and clearance and (iv) finally their therapeutic efficacy in appropriate disease model. Thus in this review, we will discuss the various clinical applications of gold, silver and platinum nanoparticles with relevance to above parameters. We will also mention various routes of synthesis of these noble metal nanoparticles. However, before we discuss present research, we will also look into the past. We need to understand the discoveries made before us in order to further our knowledge and technological development.

### I. Historical Perspective

Precious metals have a long and rich history of use harkening back to the Egyptian First Dynasty. Gold in particular was a much sought after metal and mined as early as 2900 BCE in the deserts of Ethiopia and Nubia<sup>1</sup>. In Egypt, mineralogists soon learned to purify this metal. Since then, there has been evidence of objects made from gold from the Early Dynastic period of Ur (2500 BCE) to Babylonia. Beni Hassan, a tomb dating in the same

\*\* Part of the nanomedicine themed issue

\* Address for Correspondence: Priyabrata Mukherjee, PhD, Department of Biochemistry and Molecular Biology, Department of Biomedical Engineering, Cancer Center, Gugg 1321B, College of Medicine, Mayo Clinic, 200 First St SW, Rochester, MN 55905, Mukherjee.priyabrata@mayo.edu.

era, has representative inscriptions of the extraction process from quartz matrix and gold ores in addition to the weighing and melting processes<sup>2</sup>. 2000 years later, Darius, the king of Persia (558-486 BCE), was reported to have received unrefined gold and gold dust as gifts from the Ethiopians<sup>3</sup>. The early fascination with metals is further illustrated by the keen interest of early alchemy philosophers who believed in the spiritual connection between the seven metals: gold, silver, mercury, lead, tin and iron, with the seven heavenly bodies: the Sun, the Moon, Venus, Jupiter, Mercury, Saturn and Mars<sup>2</sup>. It was believed that Earth housed the seeds of metals and was under the influence of the heavenly bodies (Fig. 1).

For alchemists, gold was greatly treasured as evidenced by the common quest for the philosopher's stone (*Japis philosophorum*), an agent that would make possible transmutation of base metals into gold<sup>4, 5</sup>. Furthermore, gold was considered to be indestructible and have immense medicinal value; hence early alchemists set out to produce potable gold, "the elixir of life"<sup>5</sup>. In 8<sup>th</sup> century CE, an alchemist in Arabia, Jabir ibn Hayyan, also known as "Geber" in Europe, succeeded in dissolving gold in *aqua regia*, a mixture of nitric and hydrochloric acid<sup>1</sup>. By the 7<sup>th</sup> century, gold chloride had become commonplace and in the early Renaissance, gold was recommended to purify blood and thought to have numerous medical virtues<sup>2</sup>. The first use of gold in modern medicine was in 1890 after the German bacteriologist Robert Koch discovered that low concentrations of potassium gold cyanide,  $K[Au(CN)_2]$  had antibacterial properties against the tubercle bacillus<sup>6</sup>. In the 1920s gold therapy for tuberculosis was introduced<sup>6</sup> and in 1935 Jacques Forestier reported the use of gold to treat rheumatoid arthritis<sup>7</sup>. Gold thiolates are still in use today to treat the disease. In the United States, gold sodium thiomalate and gold thioglucose are sold as Myochrysin and Solgonal respectively<sup>8</sup>. Auranofin (triethylphosphine(2,3,4,6-tetra-O-acetyl- $\beta$ -1-D-thiopyranosato-S)gold(I) are some of the newer compounds in use as antiarthritic drugs (Fig. 2. a-c). Other gold complexes have been implicated in treatment of cancer and malaria (Fig. 2d and e).

Silver has been valued throughout history as a precious metal and in ancient times it was considered to be more valuable than gold. Believing it to be feminine in nature with its white luster, silver was considered a symbol of purity. Evidence of the use of silver to make ornaments and decorations exists from as far back as 4000 BC<sup>9</sup>. Silver was oft referred to as white gold and was known to the Greeks and inhabitants of the region between the Indus and the Nile. A gold silver alloy was used to make coins by 800 BC<sup>2</sup>. Alchemists associated silver with the moon (oft referenced the element as *luna*), and hence used it to cure ailments related to the brain (hence the term lunatic). In Arabia, it was used to treat "falling-sickness" and vertigo<sup>2</sup>. Hippocrates proclaimed that silver contained medicinal properties and could cure multiple maladies<sup>10</sup>. Since silver was touted to have antiseptic properties, Phoenicians used silver vials for food storage to help prevent spoilage. Prior to the widespread use of antibiotics, silver compounds were used to help prevent infection during World War I<sup>11</sup>. In 1881, a physician named Crede used silver compounds to help prevent gonorrhea from being transmitted from the mother to new born babies<sup>12</sup>. Lunar caustic, silver nitrate amalgamated into sticks, was also used in antiquity to cauterize wounds. Silver nitrate also has a close relationship with photography. For silver, the history of the art form begins in 1727 when John Herman Schulze, a German professor first observed that silver salts turned black when exposed to light<sup>13</sup>. Silver salts were further investigated and even hundreds of years later continued to be the critical component of photographic film.

Another noble metal, platinum was discovered on the alluvial sands of the Pinto River in Columbia<sup>14</sup>. The first reported use was by Egyptians and South Americans ca. 2000 years ago<sup>14</sup>. Archeologists uncovered an ancient Egyptian box from ~720 B.C that contains hieroglyphic characters decorated with platinum bands<sup>15</sup>. The Europeans did not know of platinum until the 16<sup>th</sup> century when the Spaniards came across the element following

conquest of the lands of South America. When mining for gold in Columbia, they found lumps of platinum which they called *platina del Pinto* meaning “little silver of the Pinto river”<sup>14</sup>. Some of the samples were brought back to Europe in 1557 and studied by Italian-French scientist Julius Caesar Scaliger who concluded that the metal was not silver and in fact a new element, Platinum. Thus Julius Caesar Scaliger is widely reported to have discovered the metal. In 1735, a Spanish scientist Antonio de Ulloa rediscovered platinum in South America and in 1783 French chemist Francois Chabaneau successfully purified it thus initiating the use of the metal for decorative purposes. A famous object made from platinum in antiquity is a chalice made in 1788 for Pope Pius VI. The popularity of the metal rose in the following years and by the 19<sup>th</sup> century platinum was in high demand for use in jewelry and industrial purpose.

In 1965, Rosenberg *et al.* discovered that electrolysis using platinum electrodes inhibited division of *Escherichia coli*<sup>16</sup>. The group subsequently reported that platinum salts,  $[\text{PtCl}_6]^{-2}$ , generated via electrolysis, were responsible for the anti-proliferative action on the bacteria<sup>17</sup>. Thus began the resurgence of investigations with cisplatin, which had remained obscure since its first synthesis in 1845 by Michel Peyrone<sup>18</sup>. In 1893, Alfred Werner had already elucidated the structure of cisplatin but it wasn't until Rosenberg that the antitumor activity of cisplatin was studied and so began the reign of the “Penicillin of cancer”. After successful studies in mice, the compound entered clinical trials in 1971. In 1977 cisplatin was licensed exclusively to Bristol-Myers Squibb and by 1978 it was approved for use in the US by the Food and Drug Administration<sup>18</sup>.

In contrast to metals, metallic nanoparticles (NPs) and their use may be considered a product of modern science since the potential of nanotechnology was only realized in recent years. Yet the synthesis and use of nanoparticles (NPs) dates back to ancient times. The first evidence of metallic nanoparticles is from 2000 years ago when gold NPs were a part of ancient ayurvedic medicine in India<sup>19</sup>. 56 nm sized colloidal gold NPs, also called the *swarna bhasma* (gold ash) was mixed with honey or cow ghee and given orally to patients to treat a wide range of diseases including rheumatoid arthritis, bronchial asthma, diabetes mellitus and other diseases of the nervous system<sup>19, 20</sup>. The aesthetic property of gold NPs was later realized and exploited by the Romans. They used gold NPs to color glass; an exemplary case in point is the Lycurgus cup (Fig. 3). The colored glass and bronze cup is dated to the 4<sup>th</sup> century Roman Empire and shows a “dichroic” effect i.e the cup appears pea green in reflected light but in transmitted light it appears to be a deep wine red color<sup>19, 21</sup>. Studies conducted by the British Museum, which houses this work of art, report that the cup composite is an alloy of 70nm NPs containing 70% silver and 30% gold<sup>21</sup>. Although one can only speculate as to whether the use of NPs was purely accidental, artisans in other cultures have shown deliberate exploitation of the unique optical effect of NPs to create colorful church windows. Silver NPs were used to stain glass a yellow color<sup>22</sup> while gold NPs were used to produce a ruby red hue. In 9<sup>th</sup> century Mesopotamia, silver and copper NPs were used to give pottery gold like iridescent, metallic luster<sup>23</sup>. The Muslim culture forbids the use of gold in artistic representation and so the artisans devised a method to employ other metallic NPs to produce a gold like result. Copper and silver salts and oxides were mixed with vinegar, clay, and ochre and then applied to glazed pottery. When “cooked” at high temperatures and a reducing environment, the metals ions would reduce and migrate to the outer layer of the glaze forming a NP coat, thus producing a brilliant gold-like end product.

But perhaps the first scientific study of metallic NPs in colloidal systems and the first observation of the unique optical properties of gold NPs was by English physicist and chemist Michael Faraday in 1857<sup>24</sup>. Faraday was the first to study and report the size dependent optical properties of gold and silver colloids. Although it would be almost a

century later when the field of nanotechnology would take off, Faraday's observation that particles on the nanoscale behaved differently from its bulk was critical and fundamental discovery. In 1908 Gustav Mie studied the mathematic correlation of NP size and its optical manifestations<sup>25</sup>. In 1959, it was physicist Richard P. Feynman who, almost a century after Faraday, memorably championed the arrival of nanotechnology<sup>26</sup>. In that momentous lecture to the American Physical Society at Caltech, he said, "There's plenty of room at the bottom—an invitation to enter a new field of physics" hinting at the potential for nanoscale design to influence a wide range of fields such as optics and electronics.

The use of metal NPs has expanded in recent years following significant developments in the synthesis process. Metals like platinum and silver have long been used as industrial catalysts. German chemist Johann Wolfgang Dobereiner, who is also known as the founder of the study of catalysis, was the first to discover the catalytic capability of finely divided platinum<sup>27</sup>. In 1820, Edmund Davy an English chemist had shown that chemically reduced platinum black could promote alcohol oxidation. Dobereiner repeated this experiment a year later and made the critical observation that at the end of the conversion of alcohol to acetic acid, platinum was unaltered and available to participate in another reaction. He later went on to develop the Dobereiner lamp, which is now appreciated as the first example to use a supported catalyst, which involves a jet of hydrogen from zinc and sulphuric acid that is spontaneously ignited in the presence of platinum<sup>27</sup>. The nanoscale size of particles was later known to enhance catalytic activity of a metal; thus metals in NP form have been keenly studied as a way to cut down costs and improve catalytic efficiency. It is interesting that gold was historically considered to be catalytically inactive. But in 1985, Graham Hutchings from the University of Cardiff, UK reported that the gold ions could catalyze the hydrochlorination reaction. Similarly, Masatake Haruta, from Tokyo Metropolitan University in Japan, later observed that in NP form gold could catalyze oxidation of carbon monoxide even at low temperatures of  $-76^{\circ}\text{C}$ <sup>19</sup>. In recent years there has also been increasing interest in the use of silver NPs as antimicrobial agents. As mentioned earlier, this remarkable property of the metal was known since antiquity to Greeks who used the metal in their cooking and used it to for safe storage of water<sup>28</sup>. Modern application of nanoparticles extends even as far as restoring centuries old works of art<sup>29</sup>. Thus NPs has been involved in our life since time immemorial. Therefore in our next section we will discuss their synthesis.

## 2. Modern Synthesis of Noble Metal Nanoparticles

Synthesis of noble metal nanoparticles (Au, Ag and Pt) has exploded in the last few decades. The most popular techniques are chemical reduction, physical processes and biological methods. The physical properties of nanoparticles include size, shape, structure and composition. Each of these aspects can be altered or manipulated by varying either kinetic or thermodynamic variables in the syntheses (Fig. 4). The ability to control specific properties through minor alterations has led to a major movement in research exploration of nanoparticles as well as increased the potential for applications within the fields of catalysis, electronics, therapeutics and diagnostics. Before we discuss the therapeutic aspects of these nanoscale materials, we must first have a look at their synthesis.

### 2.1 Chemical Reduction

**2.1.1 Gold Nanoparticles**—Collidial gold synthesis has been intensively studied for centuries<sup>30, 31</sup>. The most common method of synthesis for gold nanoparticles (AuNP) is chemical reduction. The simplest of these methods is the reduction of gold salts in the presence of a reducing agent<sup>31, 32</sup>. The first documented study of the solution phase synthesis of gold colloids was in 1857 when Michael Faraday reduced gold chloride with phosphorous in an aqueous medium<sup>24</sup>. Turkevitch et al. made the next critical discovery in 1951; he developed the citrate reduction method<sup>33</sup>. This synthesis of citrate stabilized

AuNPs was based on a single-phase reduction of gold tetrachloroauric acid by sodium citrate in an aqueous medium and produced particles about 20 nm in size<sup>33</sup>. Frens et al., later refined this method in 1973 in an effort to produce AuNPs of a prechosen size<sup>34</sup>. Frens proposed modifying the ratio between the tetrachloroaurate and the trisodium citrate, a method that is still widely employed. Pursuing this strategy of simply modifying reaction conditions such as ratios<sup>34</sup>, solution pH<sup>35</sup> and solvent<sup>36</sup> has allowed for better control of the gold nanoparticle size<sup>37</sup>, however the distribution was still variable.

In 1981, the Schmid cluster  $[\text{Au}_{55}(\text{PPh}_3)_{12}\text{Cl}_6]$  was reported to have narrow dispersity ( $1.4 \pm 0.4$  nm). Unfortunately the synthesis utilized diborane gas to reduce  $[\text{Au}(\text{Ph}_3\text{P})\text{Cl}]$  and proved to be a delicate synthesis that was difficult to isolate in a pure state<sup>38</sup>. Subsequently it was discovered by Mulvaney and Giersig in 1993 that AuNPs could be stabilized using alkanethiols of various chain lengths<sup>39</sup>. The last major contribution to the field for AuNP synthesis was published in 1994 and is known today as the Brust-Schiffrin method<sup>40</sup>. This method utilizes a two-phase synthesis that exploits thiol ligands that strongly bind to gold due to the soft character of both S and Au. Initially, a gold salt is transferred into an organic solvent (toluene) with the help of a phase transfer agent such as tetraoctylammonium bromide, and then an organic thiol is added. Lastly an excess of a strong reducing agent, such as sodium borohydride is added which produces thiolate protected AuNPs<sup>40</sup>. The major advantages of this method are the ease of synthesis, thermally stable NPs, reduced dispersity and control of size<sup>41</sup>. Although the Brust synthesis was a significant step forward and has proven extremely influential in the last 17 years since its publication, it still didn't provide the monodispersed product that was so greatly sought. Nonetheless, efforts have been made to narrow the size dispersity through purification<sup>42-44</sup>, ripening<sup>45</sup>, etching<sup>42</sup> and annealing<sup>46</sup>. Through modifications to the Brust synthesis, such as variation in the pH, reactant concentration, reduction time and aqueous methanol concentration, monodispersed particles were ascertained<sup>47-56</sup>. In the last few years, many groups have focused on producing monodispersed nanoparticles by exploring possible nanoparticle formation mechanisms in order to control the size distribution. Natan et al. was an innovator for the investigation of seeded growth of gold nanoparticles using modifications on the Frens synthesis<sup>57</sup>. Bastus et al. have successfully synthesized monodispersed citrate stabilized particles through kinetically controlled seed growth (Fig. 5)<sup>37</sup>. Factors to consider for narrow size distribution are seed concentration, number of steps and secondary nucleation events<sup>58</sup>.

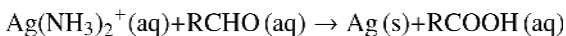
**2.1.2 Silver Nanoparticles**—Silver nanoparticles (AgNPs), though not as widely studied as gold nanoparticles, have made a remarkable impact in the world of nanoscience. Considerable effort is being directed toward developing new applications and protocols for this promising and interesting noble metallic nanoparticle. The simplest method to obtain silver nanoparticles is through a reduction of silver nitrate ( $\text{AgNO}_3$ ) in ethanol in the presence of a surfactant<sup>59</sup>. AgNPs are most commonly synthesized via chemical reduction, which is based on a two-step process<sup>60</sup>. The most widely used stabilizing agents for silver nanoparticles are polyvinyl alcohol, poly (vinylpyrrolidone), bovine serum albumin (BSA), citrate and cellulose. By the use of these stabilizers, unwanted aggregation of the particles is avoided.

The two most traditional solution phase synthesis routes are the Lee-Meisel and the Creighton methods<sup>61</sup>. The Lee-Meisel method was first published in 1982. It employed both  $\text{AgNO}_3$  and  $\text{Ag}_2\text{SO}_4$  as metal precursors and was further reduced with  $\text{NaBH}_4$ , sodium citrate, and  $\text{H}_2$  at various temperatures<sup>62</sup>. Unfortunately these procedures produced a variety of shapes and sizes. The polyol method is an alternation on the Lee-Meisel method. This method reduces silver salts with a diol solvent near reflux temperatures in the presence of a polymeric stabilizing agent. Size and shape control has been achieved with this type of

synthesis<sup>63</sup>. The Creighton method is the most common, producing particles with a fairly narrow size distribution through the reduction of AgNO<sub>3</sub> with NaBH<sub>4</sub><sup>64</sup>. Building on these pioneering methods, the Yang group used sodium citrate under a range of pH values (5.7 – 11.1) to control both the size and morphology of silver nanoparticles<sup>65</sup>. It was found that high pH created both rod and spherical particles due to a fast reduction rate silver nitrate (Fig. 6). Triangle and other polygon shapes were observed with lower pH values (5.7 – 11.1) primarily due to slow nucleation and growth<sup>65</sup>. Thus, the morphology of spherical AgNPs can be controlled via a two-step process: fast nucleation at high pH followed by slowing down the growth phase by reducing the pH.

In some instances, the reducing and stabilizing agent is one and the same. For example, polysaccharides can serve as both the reducing and capping agent. In this novel method, starch and β-d-glucose were gently heated in an aqueous solution containing silver. Due to the weak surface binding of starch to silver, the reaction is reversible at high temps, allowing for variation. Starch alone can also create stable AgNPs (10–34 nm) via an aqueous solution of silver nitrate autoclaved at 15 psi/121°C/5 minutes. In yet another example of this method, a heated solution of AgNO<sub>3</sub> and heparin was used to produce AgNPs. Through variation in heparin concentration, the AgNP size and shape can be manipulated. In this case, heparin acts as the reducer, stabilizer, and nucleating agent.

Like gold, a one step process is highly desirable for the synthesis of silver nanoparticles<sup>66, 67</sup>. Procedures to produce AgNPs of uniform size and morphology are employing a modified Tollens synthesis reaction:



In the presence of ammonia (the solvent), silver ions are reduced by polysaccharides, which yields AgNPs ranging from 50–200 nm<sup>68</sup>. The size of these particles is controlled by the 1) concentration of ammonia and 2) the nature of the stabilizer (either SDS, PVP, or Tween 80)<sup>66, 67</sup>. The mixture of glucose with 5mM ammonia produced 54 nm AgNPs<sup>66</sup>. Modifying the pH of the solvent as well as the structure of the reducing agent can further decrease size polydispersity. For example, the narrowest size distribution of AgNPs (25 nm) was formed by using maltose as the reducing agent and a pH of 11.5<sup>69</sup>.

**2.1.3 Platinum Nanoparticles**—Platinum complexes, such as cisplatin, have been used for several decades to treat a number of maladies. However, the use of platinum nanoparticles (PtNPs) as therapeutics is still in its nascent state<sup>70</sup>. The most common method for the synthesis of platinum nanoparticles is by chemical reduction of metal salts, chief among these agents are ethylene glycol and sodium borohydride<sup>71, 72</sup>. For example, Guo et al formed PtNPs using borohydride as the reducing agent and citric acid as a stabilizer<sup>73</sup>. By varying the ratio of citric acid to the metal salt, they were able to form PtNPs ranging in size<sup>73</sup>. The size and shape of PtNPs can be controlled by the precursor reduction conditions while employing supercritical fluid reactive deposition<sup>74</sup>. Herricks and co-workers describe a scheme to generate PtNPs with various morphologies<sup>71</sup>. In this method, polyethylene glycol serves as the reducer and solvent. Further variation of structure was obtained by changing the NaNO<sub>3</sub>/Pt ratio<sup>71</sup>. Additionally, platinum nanoparticles exhibit size and shape dependent catalytic properties<sup>75</sup>. Other capping agents such as poly(N-vinyl-2-pyrrolidone) have been used in conjunction with NaBH<sub>4</sub> reduction of H<sub>2</sub>PtCl<sub>6</sub>·6H<sub>2</sub>O (Fig. 7)<sup>76, 77</sup>. Finally, the size of PtNPs can be fabricated using chemical ripening<sup>78</sup>. The initial step of this multistep, multi-seed process begins with small individual platinum seeds (~ 5 nm) in an aqueous solution containing sodium citrate and L-ascorbic acid. The final diameter of the PtNPs relies on the concentration of chloroplatinic acid and the initial seed size<sup>78</sup>.

## 2.2 Physical methods

Noble metal nanoparticles can be successfully synthesized using other procedures such as UV irradiation and microwaves, which may or may not employ reducing agents. For instance, well defined (shape and size distribution) AgNPs were formed from a direct laser irradiation of an aqueous solution of silver nitrate and SDS<sup>79</sup>. In this instance, the surfactant (SDS) also acts as the stabilizer, which further tunes the size and shape of the nanoparticle. Additionally, the above technique was also utilized employing benzophenone<sup>80</sup>. By varying the time and laser power, the size of the AgNPs could be controlled; short irradiation at a low power produced ~20 nm particles whereas 5 nm particles were generated with longer irradiation times and a higher ionizing power<sup>80</sup>. Particle size can also be controlled with the duration of photolysis<sup>81</sup>. In this instance, the substrate initiates the reduction of Ag<sup>+</sup> to form silver seeds (Ag<sup>0</sup>) upon excitation at 600 nm. A further ripening process using high intensity laser excitation controlled the growth rate of the silver seeds. Uniform water-soluble silver nanoparticles (~ 26 nm) can also be formed via microwave irradiation<sup>82</sup>. This method uses basic amino acids (0.16 mmol) to reduce silver salts (20 mmol) in an aqueous starch solution (0.4 mmol), which is heated for 10 seconds at 150 °C. The rapid nucleation process, due to microwave irradiation, is critical to the uniform size distribution of the nanoparticle. Work done by Suzuki proposed a new method to fabricate monodisperse spherical AgNPs ranging from 10 to 80 nm in an aqueous solution<sup>83</sup>. This simple yet elegant method uses a combination of seeding and laser treatments (Fig. 8). The authors used “soft” irradiation: particles were heated and melted by a single laser pulse. The final diameter ( $d_p$ ) of the AgNPs can be calculated based on the assumption that the reduction of Ag<sup>+</sup> is only at the surface of the seed particle using the following equation:  $d_p/d_{p0} = (1 + n^+/n_s)^{1/3}$ . Through changing the ratio of  $n^+$  (silver ion) and  $n_s$  (seed particle), the average size of the particle can be controlled through increasing the  $n^+/n_s$  ratio.

Photochemical reduction of gold salts has also been used to form AuNPs<sup>84</sup>. This nanoformulation method employs a continuous wave UV irradiation (250– 400 nm), PVP as the capping agent and ethylene glycol as the reducing agent. The rate of formation of AuNPs with this method is dependent on the glycol concentration as well as the viscosity of the solvent mixture. This method was further improved upon by the addition of Ag<sup>+</sup> to the solution, leading to an increase in the production of Au<sup>0</sup> and the ensuing nanoparticles<sup>85</sup>. By using photochemically prepared seed particles, the size of AuNPs can be further tailored<sup>86</sup>. In this preparation, spherical particles (5 to 20 nm) were prepared with UV irradiation using various ratios of surfactant (TX-100) to gold ion concentration<sup>86</sup>. Larger particles were further formed by reducing fresh Au(III) ions onto the surface of the seeds particles in ascorbic acid. Through varying the [Au(III)]/[seed] ratio, the surface size of the particle can be controlled.

Others have applied laser-based approaches to generate spherical gold nanoparticles in the absence of a reducing agent. In one method, thermal-free femtosecond laser radiation was used to ablate gold in deionized water. Briefly, low laser fluences ( $F < 400 \text{ J/cm}^2$ ) produced 3–10 nm relatively monodispersed gold particles<sup>87</sup>. Another group used laser irradiation to elucidate the morphological changes induced by ablation, comparing size dispersion between the second (532 nm) or fourth harmonic (266 nm) of a pulsed laser<sup>88</sup>. It was established that the mean size of the AuNPs could be tuned by using the proper combination of laser ablation, laser fluence and post-irradiation wavelength. Positively charged nanoparticles can also be fabricated using pulsed laser light without the incorporation of ligands or reducing agents<sup>89</sup>. Gold foil was pulsed with a femtosecond laser (delivering 120 fs laser pulses) at 800 nm in aqueous solution for a period of 12 minutes. This method produces a surprisingly stable gold nanoparticle in a variety of media primarily due to the partial oxidation of the gold surface<sup>89</sup>.

Irradiation and laser ablation techniques have also been effectively used to create PtNPs. For instance, radiolytic reduction of platinum complexes such as  $(\text{Pt}(\text{NH}_3)_4\text{Cl}_2 \cdot \text{H}_2\text{O})$  can be stabilized with polyacrylic acid<sup>90</sup>. In another method, irradiation was combined with ultrasonication to prepare PtNPs<sup>91</sup>. In this process,  $\text{H}_2\text{PtCl}_6 \cdot 6\text{H}_2\text{O}$  was added to a solution containing 10 mM polypyrrole and SDS. By varying the length and time of irradiation and ultrasonication, the particle size is controlled<sup>91</sup>. Ablation of platinum targets in aqueous solution using a nanosecond laser has also generated PtNPs. This method, described by Cueto, used several laser wavelengths and stabilizing agents to create a range of sizes and shapes of PtNPs<sup>92</sup>.

### 2.3 Biological Methods

Numerous reducing agents have been studied, such as hydroxylamine<sup>57, 93</sup>, ascorbic acid<sup>94, 95</sup> and biogenic methods which utilizes an iodide-mediated reduction<sup>96</sup>. In addition to aforementioned synthesis, some efforts have been put forth to elucidate biological methods to produce nanoparticles. Plant mediated particle synthesis has gained momentum due to simplicity and eco-friendliness (See Table 1)<sup>97</sup>. Biosynthesis with plant extracts as well as Iodide mediated reductions of  $\text{AuCl}_4^-$  have been reported<sup>96, 98</sup>. Blood compatibility also makes green syntheses attractive<sup>98</sup>. For example, it has been shown that *Zingiber officinale* extract can produce particles ranging from 5–15 nm in diameter. The extract acts as a reducing agent as well as a stabilizer and the biological benefits are proven through physiological stability<sup>98</sup>. The use of microorganisms for synthesis has also emerged as an alternative to chemical fabrication, yielding a strong area for investigation into green syntheses. Photosynthetic bacteria<sup>99</sup>, prokaryotic bacteria<sup>100–102</sup>, eukaryotic fungus<sup>103, 104</sup> and plant extract<sup>105–108</sup> have all been employed for the reduction of aqueous metal ions to produce metallic nanoparticles. Many biological methods have a slow reaction rate and a wide distribution in particle size<sup>109</sup>. However, a recent publication by Darroudi investigated the role of sodium hydroxide as an accelerator to generate AgNPs<sup>110</sup>. Briefly, silver nitrate, sodium hydroxide and gelatin were mixed and then heated to 60°C. After adding glucose, the reaction was allowed to stir for an additional 15 minutes. It should be noted that the size of the formed AgNPs was dependent on the volume of NaOH used. This method yielded fairly monodispersed silver nanoparticles under 20 nm in size.

In summary, optimizing nanoparticle synthesis is a prolific area of research. Controlling size, shape, and distribution is an elegant and arduous process. These reactions are ruled by many variables such as reactant concentration, solubility, reaction rate, reduction potential, temperature and time. All of the parameters are intrinsically intertwined. Further investigation is certain to be an ongoing area for increased tunability.

## 3. Therapeutic Applications of Noble Metal Nanoparticles

Nanoparticle (NP) biotechnology is a burgeoning field with immense potential for clinical and real world applications. To realize this potential, especially in therapy it is necessary to design and engineer NPs that can be targeted to tissues of interest, as well as to produce specific, desired effect (with minimal toxicity and environmental impact). Of particular interest are NPs with a metallic core due to their purported favorable safety profile in humans (indeed, colloidal metal has seen medicinal use since ancient times), which has already resulted in preclinical testing for imaging, diagnostic and therapy. Defining the size of a nanoparticle is somewhat obscure and debatable, with the colloquial designation being less than 1  $\mu\text{m}$  in diameter. Accordingly, the size of the nanoparticles used in the field of bionanotechnology range from 2 nm to 500 nm. Given that systems at these molecular and atomic scales display essentially new properties due to their small structure, innovative molecular design can be precisely created along with a high degree of versatility. This



tailoring is largely due to “self-assembly” of the nanoscale materials via charge compatibility and non-covalent interactions.

As mentioned previously, nanoparticles, have proven to be the most versatile and widely used constituents with broad applications such as delivery vectors<sup>111</sup>, imaging agents<sup>112</sup>, synthetic inhibitors<sup>113</sup>, and sensors<sup>114</sup>. Thus these engineered nanomaterials serve as unique multi-dimensional scaffolds that vary from their bulk counterpart<sup>115</sup>. Inorganic nanomaterials in particular are very attractive for various biomedical applications due their size and shape dependent optoelectronic properties<sup>116, 117</sup>. The use of nanoparticles in biology, takes advantage of both the dimension and function of the inorganic core, which in turn dictate certain physical properties<sup>116, 118</sup>. For instance, the superparamagnetism of iron oxide and iron-platinum nanoparticles and the size-dependent fluorescence of semi conductor nanoparticles are intrinsic to these particular nanomaterials<sup>116–118</sup>. Furthermore, the size of these nanomaterials provides a large surface area to volume ratio; as the particle size decreases, the amount (or number) of surface atoms rapidly increase<sup>116, 118</sup>. Through exploiting these extraordinary properties, nanoparticle therapeutics can offer an alternative platform for a wide variety of human maladies in clinical settings<sup>116, 119, 120</sup>.

### 3.1 Cellular Uptake of Noble Metal Nanoparticles

The cellular internalization of inorganic nanoparticles is an area of intense research. Even though gold, silver and platinum nanoparticles are noble metals, their mechanism of intracellular uptake is not necessarily similar or well understood. For instance there is contrasting evidence on the uptake mechanisms of AuNPs. Geiser *et al.* used red blood cells to elucidate intracellular uptake of gold nanoparticles<sup>121</sup>. Their results support a diffusive mechanism of entry since AuNPs were found in the cytosol free from membrane encapsulation (ie. endosomes). In comparison, it has been indicated that cellular uptake of AuNPs is due to macropinocytosis<sup>122</sup> which was later confirmed by further research in other groups<sup>123</sup>. Macrophages also easily internalized AgNPs, which were found to localize to vacuoles within the cells, however the authors were unable to discern the mechanism of internalization<sup>124</sup>. In an analogous study by Yen *et al.*, they showed that AuNPs and AgNPs were confined in cytoplasmic vesicles of the macrophages<sup>125</sup>. However the authors further speculated that the protein corona formation influenced cellular internalization of AuNPs, compared to AgNPs, thus complicating the uptake process<sup>125, 126</sup>. Original work from Taylor and coworkers analyzed the cellular uptake of gold nanoparticles generated via laser ablation<sup>89</sup>. In this study, the authors cultured bovine cells (GM7373) with the AuNPs (15 nm, 50  $\mu$ M) in a time course study. With the aide of confocal microscopy, they were able to determine that the AuNPs were passively taken up via diffusion through the cellular membrane<sup>89</sup>. This is in contrast to gold nanoparticles created through chemical means, which seem to prefer endosomal transport<sup>123, 127, 128</sup>. It may also be possible to tailor the endocytotic uptake of nanoparticles. In a very recent study, Bhattacharyya *et al.* shows that the endocytotic pathway can be “switched” from a caveolar mechanism to pinocytosis<sup>129</sup>.

The size and shape of nanoparticles also play a large role in relation to cellular uptake *in vitro*. Spherical gold nanoparticles have higher cellular uptake than gold nanorods owing to variable biophysical properties such receptor diffusion kinetics<sup>130</sup>. The extent of nanoparticles exocytosis is a function of nanoparticle surface size<sup>130</sup>. For instance, 14 nm particles were rapidly cleared from cells twice as fast as 100 nm particles. Finally, cellular uptake of metallic nanoparticles has also been reported to be size specific, with 40 – 50 nm having the greatest effect on internalization into cells<sup>131–133</sup>. Chan et al has reported that 50 nm gold particles can enter into cell at a faster rate with higher amount relative to the other sizes<sup>130</sup>. In addition they also show that the morphology of the particle also dictates the rate of cellular uptake<sup>130</sup>. The size of monodispersed nanoparticles can also be influenced by its surroundings, ie biological media. In a new study by Albanse and Chan, they describe the

interaction of aggregated nanoparticles with three different cell lines (HeLa, A549, and MDA-MB 435) *in vitro*<sup>134</sup>. The aggregation of nanoparticles is primarily due to the amount of ions found in biological medium<sup>135, 136</sup>. Upon exposure, the electrostatic nature of the nanoparticles is weakened and van der Waals forces take over<sup>135</sup>. Furthermore, a more thermodynamically favorable serum protein may displace the nanoparticle-capping agent. It is primarily these destabilizing processes that create nanoparticle aggregates in biological fluids (saliva, cell culture medium, lung surfactants). This inevitable nanoparticle aggregation creates a multitude of cellular responses<sup>134</sup>. The results of this study showed the uptake into HeLa and A549 cells was decreased by 25% with aggregated nanoparticles versus monodispersed particles. In contrast, the uptake of aggregates into MDA-MB 435 cells demonstrated a two-fold increase comparatively. Kudgus and coworkers also showed size dependent nanoparticle uptake *in vitro* and *in vivo* in an orthotopic model of pancreatic cancer. Pancreatic cell lines (AsPC-1, PANC-1, and MiaPaca-2) were co-incubated with gold nanoparticles with varying hydrodynamic radii (7 nm to 134 nm). Upon gold analysis, nanoparticles with a ~20 nm hydrodynamic radii exhibited the greatest uptake. Interestingly enough, the outcome of their *in vivo* experiments mirrored their *in vitro* results. Most importantly, Kudgus' study elucidated the design parameters for nanoparticle therapeutics<sup>32</sup>.

Surface charge is also an important factor that moderates cellular uptake of nanoparticles<sup>137, 138</sup>. The functionality of the nanoparticle surface further allows specific or nonspecific interactions within the cellular lipid bilayer<sup>32</sup>. Since the cellular exterior is largely anionic, positively charged nanoparticles can easily transverse the cellular membrane via electrostatics<sup>137</sup>. Nonetheless, negatively charged nanoparticles have also been observed in the cytosol<sup>138</sup>. This is most likely due to the nanoparticles passively targeting lipophilic domains. In a previous report, it is described that the structure and order of capping agents on nanoparticles mitigates cellular uptake<sup>139</sup>. Cationic nanoparticles have also been shown to modulate membrane potential of cells and their subsequent downstream intracellular events. In the findings published by Arvizo *et al.*, ovarian cancer and airway cells co-incubated with positive nanoparticles depolarized the cell membrane and triggered the release of intracellular calcium<sup>140</sup>. The effect was shown to be dependent on the cell type. For instance, inhibition of proliferation was observed in airway cells but the malignant cells remained unchanged. Furthermore, there are other reports where proteins in the serum help facilitate nanoparticle uptake into cells<sup>141</sup>. In addition, the Rotello group has also reported that zwitterionic nanoparticles (effective overall neutral surface charge) can be highly efficient delivery system<sup>142, 143</sup>.

There have been a few publications that have investigated the intracellular compartmentalization of nanoparticles. Silver nanoparticles have been found in the cytoplasm and mitochondria of primary liver cells as well as the mitochondria and nucleus of fibroblasts<sup>144, 145</sup>. In keratinocytes, silver was found to be localized to lysosomes, while lung cancer cells exposed to AgNPs with different sugar coatings were found in the cytoplasm<sup>146</sup>. It was further noted that the rate of uptake was dictated by the surface coating, with lactose having the greatest effect on the rate of internalization in fibroblasts<sup>147</sup>. In addition, Lesniak *et al.* found silver within endocytic vesicles<sup>148</sup>. AgNPs have also been purported to use macropinocytosis and clathrin mediated uptake in NIH3T3 cells, appearing in the cytoplasm as well as the nucleus<sup>145, 149</sup>. It was also further implied that AgNPs are directly toxic to the cancer cells through DNA damage and increased production of reactive oxygen species<sup>149</sup>. Breast cancer cells (MCF-7) treated with colloidal silver lead to dose dependent apoptosis (LD<sub>50</sub> of 3.5 ng/ml) and a significant increase in SOD activity but did not affect the viability of normal PBMC cells<sup>150</sup>. Further analysis of the intracellular uptake of AgNPs done by Greulich and co-workers, using scanning electron microscopy, detected nanoparticle aggregates in human mesenchymal stem cells<sup>151</sup>. Upon staining of the mesenchymal cellular structures, the AgNPs agglomerates were located in endo-lysosomal

structures, but not in the cellular nucleus or other cellular organelles<sup>151</sup>. Platinum nanoparticles were also detected in intracellular vesicles in the cytoplasm of HT29 cells using bright field electron microscopy<sup>74</sup>. Although there is evidence that Pt-NPs affects the integrity DNA, the intracellular redox status of HT29 cells was not altered<sup>133</sup>.

### 3.2 Nanoparticles as anti-infective agents

The function of silver nanoparticles as antibacterial agents has been well established and will not be covered further in this review. However, little has been written on the role of nanoparticles as anti-virals. In one study, it is indicated that the anti-viral properties of AgNPs biogenically formed are more effective than chemically synthesized silver nanoparticles<sup>152</sup>. Likewise, Vero cells co-incubated with AgNPs were reported to prevent plaque formation after being infected with the Monkeypox virus<sup>153</sup>. Metallic nanoparticles have also been described as a possible HIV preventative therapeutic<sup>154, 155</sup>. In a couple of studies, it is demonstrated that AgNPs prevented the virus from binding to the host cells *in vitro*<sup>156, 157</sup>. It was further shown that silver acts directly on the virus as a virucidal agent by binding to the glycoprotein gp120<sup>89</sup>. This binding in turn prevents the CD4-dependent virion binding which effectively decreases HIV-1's infectivity<sup>158</sup>. Metallic nanoparticles have also been effective antiviral agents against herpes simplex virus<sup>159</sup>, influenza<sup>160</sup>, and respiratory syncytial<sup>161</sup> viruses.

### 3.3 Anti-Angiogenic Properties of Metallic Nanoparticles

It is well recognized that angiogenesis plays a central role in a number of diseases such as cancer, rheumatoid arthritis, and macular degeneration<sup>162–164</sup>. In normal conditions, angiogenesis is tightly regulated between various anti-angiogenic (i.e. TSP-1, platelet factor 4) and pro-angiogenic growth factors (i.e. VEGF, PDGF, TGF- $\beta$ )<sup>165</sup>. However, when the balance is disrupted under pathological conditions, the angiogenic switch is turned on<sup>165</sup>. This event induces highly abnormal blood vessels which, become hyperpermeable to plasma proteins. Some anti-angiogenic agents are being presently used in the clinics, but a majority of them have been designed to only inhibit VEGF<sub>165</sub> mediated signaling<sup>166</sup>. In addition, other reports have indicated unexpected and serious toxicities of these conventional agents including hypertension, thrombosis, and fatal hemorrhage<sup>162, 163</sup>. Furthermore, relevant clinical data indicates that targeting a single pathway is not the most efficient or effective mode of treatment<sup>167</sup>.

**3.3.1 Applications in Tumor Therapy**—Owing to the above concerns, noble metal nanoparticles might prove to be more effective since they have been shown to target multiple pathways<sup>168</sup>. More importantly, the unusual toxicities associated with conventional anti-angiogenic agents (as mentioned prior) may be overcome if these nanoparticles alone can be efficacious as an anti-angiogenic agent. In a landmark study, it was shown that “naked” gold nanoparticles inhibited the activity of heparin-binding proteins, such as VEGF<sub>165</sub> and bFGF *in vitro* and VEGF induced angiogenesis *in vivo*<sup>169</sup>. However, non-heparin binding proteins, (VEGF<sub>121</sub> and EGF) retained their intrinsic activity. Further work in this area elucidated that heparin-binding proteins are absorbed onto the surface of AuNPs<sup>170</sup> and were subsequently denatured<sup>171</sup>. The researchers also showed that surface size, not surface charge, plays a large role in the therapeutic effect of AuNPs<sup>171</sup>. In this study, Arvizo and coworkers preincubated VEGF 165 with citrate reduced AuNPs (d = 5, 10, and 20 nm) to determine their effect on downstream signaling in HUVEC cells (Fig. 9). The data demonstrated that 20 nm citrate reduced AuNPs had a dramatic effect on VEGF signaling events such as receptor-2 phosphorylation, intracellular calcium release, and proliferation comparatively. Mukherjee and colleagues also tested the effect of gold nanoparticles on VEGF mediated angiogenesis using a “mouse ear model” injected with an adenoviral vector of VEGF (Ad-VEGF – mimics the resulting angiogenic response found in

tumors)<sup>169</sup>. A week after the Ad-VEGF administration, mice treated with AuNPs developed lesser edema than the sham treated mice.

Silver has also been shown to exhibit anti-angiogenic effects. In a report by Eom and colleagues, 40 nm silver nanoparticles (AgNPs) were used to study their antiangiogenic properties in bovine retinal epithelial cells (BREC) *in vitro* and a matrigel plug assay *in vivo*<sup>172</sup>. The outcome of their experiment showed that AgNPs inhibited cell proliferation and migration in VEGF induced angiogenesis in BRECs. Thus it is implied that the PI3K/Akt signaling pathway is in some way targeted and activated by AgNPs<sup>172</sup>. They went on to reveal the formation of new blood vessels was suppressed by AgNPs *in vivo*. Further work done by this group also described the anti-tumor effects of 50 nm AgNPs *in vitro* and *in vivo*<sup>173</sup>. Dalton's lymphoma ascites (DLA) cell lines co-incubated with AgNPs displayed a dose dependent toxicity through activation of caspase-3 and inhibition of cellular proliferation. Furthermore, tumor bearing mice injected with AgNPs demonstrated a reduction of ascites production (65%) and tumor progression compared to the sham treated mice<sup>173</sup>.

**3.3.2 Applications in Multiple Myeloma**—The pathogenesis and progression of multiple myeloma (MM) can also be attributed to abnormal angiogenesis<sup>174, 175</sup>. Even with intense study, this malignancy of plasma cells remains fatal. Current research proposes that the rise of angiogenic activity of the myeloma cells is due to the increased expression of cytokines including bFGF, VEGF, hepatocytes growth factor (HGF), insulin like growth factor (IGF-1), and TGF- $\alpha$ <sup>176</sup>. Treatment strategies used in the clinics include a combination of chemotherapy either alone or with stem cell transplantation, glucocorticosteroids, thalimide, and proteome inhibitors (such as Bortezomib)<sup>175</sup>. Unfortunately, these treatments are not restorative and the majority of patients go into relapse. As mentioned above, work done in the Mukherjee group demonstrated that gold nanoparticles inhibited the inherent function of heparin binding growth factors<sup>169–171</sup>. These studies led to the hypothesis that gold nanoparticles could also inhibit the VEGF and bFGF dependent proliferation of MM cells. In all three cell lines tested (OPM-1, RPMI-8266, and U-266), a dose dependent inhibition of proliferation was observed in AuNP treated samples (with no inhibition of normal cells at sub toxic levels of AuNPs)<sup>177</sup>. Further cell cycle analyses revealed an arrest in the G1 phase of the cell cycle, with an up-regulation of p21 and p27. This study is an important first step in show casing the potential of AuNPs as a therapeutic moiety in the treatment of multiple myeloma.

**3.3.3 Applications in Leukemia**—B-chronic lymphocytic leukemia (B-CLL) is the most widespread form of leukemia. Primarily found in males, this disease affects B-lymphocytes and causes infiltration of malignant cells into organs as well as immune suppression. Not surprisingly, abnormal angiogenesis was detected in the marrow of B-CLL patients with a significant increase in the marrow vasculature<sup>178</sup>. Supporting these observations, it was found that patients with this disease also had a substantial amount of bFGF and VEGF in their urine<sup>178</sup>. The biological component of this disease was further confirmed with clonal cell studies of B cells from patients; higher levels of bFGF resisted the apoptotic effects of the drug fludarabine<sup>178</sup>. The anti-angiogenic properties of AuNPs stated earlier, led to the possibility that the status of B-CLL cells could also be modulated by AuNPs<sup>178</sup>. Indeed, B-CLL cells exposed to gold nanoparticles exhibited an increase in apoptosis in a dose dependent manner. The mechanism of apoptosis enhanced by gold nanoparticles in B-CLL cells was further elucidated by a clearly detectable PARP cleavage and a decrease in anti-apoptotic regulatory proteins such as caspase-3, Bcl-2 and Mcl-1<sup>178</sup>.

**3.3.4 Applications in Rheumatoid Arthritis**—Angiogenesis also plays a large role in the promotion and maintenance of inflammatory diseases such as rheumatoid arthritis (RA).

Historically gold salts have been used to treat a multitude of inflammatory diseases (see Fig. 3) <sup>179</sup>. Clinicians first started using gold complexes the early 1900s to help treat rheumatoid arthritis <sup>180</sup>. However these gold(I) thiolates needed to be injected and the response to treatment took several weeks to months with patients incurring several adverse side effects <sup>181</sup>. In 1985, the oral drug Aurofin (Ridauro™) was introduced as a safe and effective treatment for RA <sup>179, 180</sup>. However, it was later shown to be less effective than the original thiolates <sup>8</sup>. In a current study, 13 nm gold nanoparticles were used to study rats with collagen-induced arthritis <sup>182</sup>. Initial studies showed that the nanoparticles bound to VEGF in the synovial fluid of patients with RA affecting cellular proliferation and migration. Subsequent histology from animal models showed that TNF- $\alpha$  and IL- $\beta$  was considerably reduced after intraarticularly administration of the nanoparticles. Moreover, AuNP treatment resulted in further attenuation of arthritic symptoms such as inflammation and reduced macrophage infiltration. In a related study, gold beads were implanted near the hip joints of dogs with hip dysplasia in a double blind clinical trial <sup>183</sup>. After a 24-month period, 83% of the dogs in the treatment group showed continuous pain relief from the implantation compared to the placebo group <sup>183</sup>.

### 3.4 Applications for Anti-Tumorigenesis

**3.4.1 Hyperthermia/photothermal therapy**—A combination of surgery, chemotherapy, and radiation therapy constitutes the conventional treatment regime for most cancers. Although successful in many instances, these treatments are responsible for significant damage to healthy tissue, with concomitant health-related issues <sup>168</sup>. These issues arise in part from the “whole-body” approach of these therapies. To minimize the damage of non-cancerous tissue, treatments could be applied directly to the tumor, leaving neighboring tissue unaffected. Two types of targeting can be used to enhance the efficiency of tumor therapy. First, the tumor can be targeted spatially, with the toxic effect of the therapeutic agent localized to the tumor site. The second type of targeting is on the cellular level. By targeting the treatment directly to tumor cells, other cells in the vicinity of the tumor will not need to be sacrificed <sup>184</sup>. In this regard, metallic nanoparticles have potential for non-invasive tumor treatment <sup>185</sup>. Application of a magnetic field will selectively heat the nanoparticles rapidly and efficiently, allowing for selective destruction of tumor cells <sup>185</sup>.

Current areas of research being actively pursued to localize cancer treatment to affected regions of the body include photodynamic therapy (PDT) and regional hyperthermia <sup>184, 186–189</sup>. Targeting is primarily achieved by focusing the light source on a region of the body. The wavelength of light that is readily absorbed by tissue is 630–900 nm, otherwise known as the near infrared region (NIR) <sup>186</sup>. This spectral region minimizes the light extinction by intrinsic chromophores in the healthy tissue <sup>190</sup>. Another method of restricting healthy tissue damage in tumor therapy is through regional hyperthermia <sup>187–189</sup>. In general, hyperthermia is characterized by the damage of cells from exposure to elevated temperatures <sup>189</sup>. Loss of membrane integrity, DNA damage and biochemical pathway inhibition have been implicated as causes of cellular death under these conditions <sup>191</sup>. A moderate rise in homeostatic temperature has been shown to induce apoptosis within a few hours. As temperatures rise above 46°C, necrosis is observed <sup>192</sup>. Although potentially useful, this technology is limited by the difficulties in achieving a localized, uniform heating of tissue (Fig. 10).

Recent innovations in nanotechnology have demonstrated that metallic nanoparticles hold great promise as PDT and hyperthermic agents. Research has shown the application of magnetic fields on metallic nanoparticles results in rapid heating <sup>193</sup>. In this heating process, electrical currents are produced in the gold particle by the oscillating magnetic field, analogous to the current provided by an electrical generator <sup>193, 194</sup>. The resulting eddy

currents create this rapid heating which quickly dissipates from the nanoparticle into the surrounding environment, incurring thermal ablation<sup>195</sup>. Pioneering work by Pitsillides illustrated that the surface plasmon resonance (SPR) of nanoparticles is easily exploited for PDT anti-cancer therapy<sup>196</sup>. Further work done in the El-Sayad group demonstrated that AuNPs are effective PDT agents and could “seek and destroy” cancerous cells<sup>187</sup>. A four-minute exposure at 25 W/cm<sup>2</sup> was lethal to malignant cells, a two-fold decrease in comparison to normal cells (57 W/cm<sup>2</sup>). In a fairly recent report, 15 nm citrate capped AuNPs were used to treat A431 cells using photothermal therapy (PTT). In this study, AuNPs were exposed to low laser light at different time intervals and the morphology of the A431 cells was assessed along with germane biological markers. After irradiation, it was shown that AuNPs induced the eradication of the malignant cells through ROS mediated apoptosis<sup>197</sup>. It should also be noted that the shape of the particle is also important in PDT therapy. In a report by the Kanaras group, gold nanoparticles with different morphologies were incubated with HUVEC cells and their uptake after laser irradiation was investigated<sup>198</sup>. It was implicated from their results that gold nanorods were taken up 100 times more than the other particles studied. However, they noted that each particle was uniformly efficient in promoting cell death when laser hyperthermia is employed.

Likewise, mice injected with gold nanoparticles had a significant reduction of deep tissue tumors after a brief exposure to NIR<sup>199</sup>. Local laser induced hyperthermia has also been employed against skin cancer<sup>200</sup>. In this study, AuNPs were injected into the tail vein of mice for 5 days. Within 4–5 hours, the nanoparticles accumulated into skin tumors and showed complete inhibition<sup>200</sup>. A more efficient method for penetrating deeper solid tumors is to use radio waves, or radio frequency ablation (RFA)<sup>201</sup>. At ~14 MHz, AuNPs were described to thermally ablate cancer cells and tumor tissue *in vitro* and *in vivo*<sup>202</sup>. Liver cancer cells (HepG2) co-incubated with citrate reduced AuNPs (13 nm) demonstrated a time-dependent cytotoxic effect upon exposure to the RF field. The authors were able to further correlate their *in vitro* results *in vivo* using a rat hepatoma model. Following RF exposure, rats that were injected with nanoparticles revealed evidence of thermal injury to the diseased tissue<sup>202</sup>.

The frequency of the surface plasmon band (SPR) can be tuned by changing the shape of nanoparticles to a rod<sup>203</sup>. One of the advantages of gold nanorods is the duality of the observed plasmon band that is tunable through its aspect ratio. Second, the nanorods can be tailored further owing to the distinctive surface chemistries along their crystal faces<sup>203</sup>. Moreover, the shift of the SPR allows for near-infrared (NIR) absorption at the cross-sections, permitting a deeper penetration into living tissues<sup>199</sup>. Utilizing these properties, von Maltzahn et al. have developed nanorods that target and reduce tumors<sup>204</sup>. In this study, PEGcoated nanorods were injected into the tail veins of tumor bearing mice. The treated mice were then exposed to NIR and after 15 days showed a significant reduction in tumor size. Expanding on their work, the authors tagged the nanorods with SERS reporters and demonstrated their effectiveness at imaging and ablating tumors *in vivo*<sup>199</sup>.

**3.4.2 Application in Radiotherapy**—Another common treatment for patients with cancer is the use of ionizing radiation. Although this method is effective for controlling the proliferation rate of cancer cells, it can be invasive, side effects are numerous and healthy tissue is often damaged. Metallic nanoparticles may offer an advantage in this area by exploiting their excellent optical properties, surface resonance, and wavelength tunability. For example, upon X-ray irradiation, gold nanoparticles can induce cellular apoptosis through the generation of radicals<sup>205</sup>. This treatment strategy has increased the killing of cancer cells without harming the surrounding healthy tissue<sup>206, 207</sup>. X-ray irradiation of mice injected with AuNPs at 250 kV caused a four fold decrease in tumor size and enhanced survival of the animals<sup>208</sup>. Likewise, the intrinsic radioactive properties of Au-198 ( $\beta_{\text{max}} =$

0.96 MeV;  $t_{1/2} = 2.7$  d) and Au-199 ( $\beta_{\text{max}} = 0.46$  MeV;  $t_{1/2} = 3.14$  d) nanoparticles makes them ideal candidates for radiotherapy<sup>209</sup>. Furthermore, these particles have revealing gamma emissions for dosimetry and pharmacokinetic investigations<sup>209</sup>. Gannon *et al.* reported the destruction of human cancer cells (Hep3B and Panc-1) via radiofrequency thermal heating of non-targeted AuNPs ( $d = 5$  nm)<sup>210</sup>. Treatment with 67  $\mu\text{M/L}$  of AuNPs and subsequent exposure to 13.56 MHz RF field resulted in a >96% lethal injury to the cancerous cells.

Numerous studies have elucidated to the effects nanoparticles elicit upon cellular uptake under standard cell culture conditions. For translational purposes of nanoparticles into clinical trials, systematic studies are needed to assess the nanoparticle-cell interaction after ionizing radiation (IR). In one report, researchers analyzed the uptake of nanoparticles (~5 nm) in mice colorectal adenocarcinoma tumor cells (CT26)<sup>211</sup>. Using transmission electron microscopy in conjunction with confocal microscopy, it was revealed that the absorption of the nanoparticles enhanced radiation induced cellular damage<sup>211</sup>. These findings were later substantiated by another group studying breast cancer<sup>207</sup>. Even though the intracellular uptake of nanoparticles was similar for both the cancer cells (MCF-7) and normal cells (MCF-10A), after irradiation cellular viability was significantly reduced (40%)<sup>207</sup>. These results confirmed 1) that irradiation enhances the killing effect of nanoparticles and 2) low doses of radiation can be used effectively thus decreasing localized damage to the normal surrounding tissue<sup>207,211</sup>. In a more recent study, biocompatible gold nanoparticles were used to systematically study the survival rates of EMT-6 and CT26 cells after irradiation of 10 Gy from various sources: x-ray emitter (from 6.5 keV to 6 MeV), synchrotrons, a laboratory generator, an animal irradiator, an oncology linear accelerator as well as a proton emitter widely used for therapy<sup>212</sup>. After irradiation, the percentage of cell survival decreased in a dose dependent manner, however these results were not significant<sup>212</sup>. The relative biological efficacy of proton beam therapy in prostate cancer was increased by 20% with the internalized gold nanoparticles<sup>213</sup>. Work done by Xu and coworkers demonstrated dose and size dependent cytotoxicity of glioma cells when treated with silver and gold nanoparticles, with 20 and 50 nm nanoparticles being the most effective at low radiation doses<sup>214</sup>. They further theorized that the increased sensitivity to irradiation is due to the release of  $\text{Ag}^+$  from the nanoparticle. With its ability to capture electrons,  $\text{Ag}^+$  functions as an oxidizer thus increasing production of intracellular reactive oxygen species<sup>214</sup>. Additional work in this area has shown that the surface size of AgNPs enhances the thermal sensitivity of glioma cells<sup>215</sup>. The size and the amount of particle uptake into cells also affect its radiosensitization. This was elegantly demonstrated in a recent report using nanoparticles ranging in size from 14–74 nm<sup>216</sup>. As anticipated, 50 nm AuNPs displayed the utmost enhancement factor (REF) compared to 14 and 74 nm particles (1.43 vs 1.20 and 1.25 @ 220 kVp respectively).

A novel experiment performed by Porcel *et al.* indicates that platinum nanoparticles may have potential as an alternative therapeutic for the treatment of cancer<sup>90</sup>. The combination of Pt-NPs with hadron therapy resulted in enhanced DNA strand breakage. The fast carbon ion irradiation of platinum led to the production of  $\text{OH}^-$  radicals thus amplifying the lethal damage to DNA<sup>217</sup>. Human colon carcinoma cells (HT29) showed a dose and time dependent response when exposed to platinum nanoparticles (Pt-NP)<sup>133</sup>. It was further confirmed that  $\text{Pt}^{2+}$  ions are released from the Pt-NP (from cellular endosomes) thus causing significant DNA damage and cellular apoptosis<sup>74, 218</sup>. Thus it is hypothesized that since Pt-NPs do not directly interact with DNA, the soluble species of Pt forms a complex with DNA similar to that of cisplatin<sup>74</sup>.

The effects of radiotherapy has improved by exploiting the enhanced permeability and retention effect (EPR) of interstitial tumors<sup>219</sup>. The periphery of solid tumors is often the

site of angiogenesis, which in turn induces hyperpermeability. With gaps up to 600 nm, nanoparticles could passively extravasate into the interstitial space and potentially into the hypoxic center of the tumor<sup>219</sup>. The landmark study by Paciotti was the driving force in the field to augment the efficacy of radiotherapy through metallic nanoparticles<sup>220</sup>. In a more recent study, mice bearing A431 squamous tumors were intravenously injected with <sup>111</sup>In-labeled pegylated 20-nm, 40-nm, or 80-nm AuNPs at a dose of 150  $\mu$ Ci/mouse<sup>221</sup>. Upon analysis of the intra-tumoral distribution, the 20 nm AuNPs showed higher tumor uptake and extravasation from the tumor blood vessels than did the 40- and 80-nm AuNPs. Moreover, the smaller particles presented the lowest uptake in the RES and had an increased circulation residence time<sup>221</sup>.

## 4. Pharmacokinetics, Biodistribution, and Toxicology Profiles

To realize their vast potential and clinical application, the whole body effect of noble metallic nanoparticles need to be assessed prior to clinical use. Studies evaluating the pharmacokinetics, biodistribution and possible toxicities (*in vitro* and *in vivo*) are needed to understand the broad spectrum of tolerance and the possible side effects of nanomaterials. The size, shape and ligand formulation of these nanomaterials can further alter their uptake and behavior in biological systems as discussed above. Notwithstanding, the high surface to volume ratio of nanoparticles, and unique physiochemical properties may also play a role in nanoparticle toxicity. Hence this section will discuss the effects that these nanoscale materials have on biological systems as well as the impact experienced by the surrounding environment.

### 4.1 *In vitro* studies

There are several discrepancies regarding the safety profile of gold nanoparticles based on *in vitro* cellular assays. The majority of these studies maintain that nanoparticles are fairly non-toxic<sup>222, 223</sup>. Incubation of citrate capped gold nanoparticles (10 nm) with immune cells (dendrites) did not alter the immunocellular phenotypes, activation and cell death after 48 h treatment, even with a significant amount of internalization of the nanoparticles. Though there was no apparent cytotoxicity, the cytokine profile (IL-1, IL-6, IL-10 and IL-12) was considerably changed after gold uptake implicating the modulation of the immune response as a result of nanoparticle treatment<sup>222</sup>. The Dechent group reported that 15 nm AuNP was fairly unreactive (even at 6.3 mM) compared to 1.4 nm particles, stabilized with triphenylphosphine<sup>223</sup>. The smaller (1.4 nm) AuNPs triggered cellular necrosis (IC<sub>50</sub> = 36  $\mu$ M) causing mitochondrial disruption and ROS generation, whereas the other particles did not display any notable toxicity. Addition of reducing compounds such as glutathione and N-acetyl cysteine, ameliorated the cytotoxicity of 1.4 nm AuNP. Likewise gene array analysis revealed that stress related genes were significantly upregulated upon 12 h treatment with 1.4 nm particles, but not with 15 nm particles<sup>223</sup>. In contrast, Ng *et al.* reported the effect of epigenetic modulation generated by 20 nm gold nanoparticles in lung fibroblasts<sup>224</sup>. Gold treatment caused a modification in gene expression levels with an up-regulation of microRNA-155 and down regulation of the PROS-1 gene. Albeit, AuNP treatment did not alter the DNA methylation of the PROS-1 gene, rather chromatin condensation was observed in the nucleus by TEM analysis<sup>224</sup>. An analogous study by Li and colleagues reported that 20 nm gold nanoparticles can trigger oxidative stress and autophagy in human lung fibroblasts<sup>225</sup>. The AuNP treatment also enhanced lipid peroxidation levels as evidenced by malondialdehyde (MDA) adducts and upregulation of many autophagy related gene (ATG-7). Furthermore, the authors observed autophagosome formation, specifically the increase of inflammatory enzyme cyclooxygenase-2 (COX-2) and PNK (polyneucleotide kinase 3'-phosphatase) gene production<sup>225</sup>. The Goering group investigated the biological effect of 60nm AuNPs in murine macrophage cells<sup>226</sup>. Though TEM images demonstrated AuNPs in intracellular vesicles, the cells did not elicit a pro-



inflammatory response. In a report by Schaeublin et al, keratinocytes (HaCaT) were exposed to 1.5 nm AuNPs of varying charge (positive, negative, neutral)<sup>227</sup>. Following exposure to the three different AuNPs, there was a noticeable disruption of cell morphology in a dose dependent manner<sup>226</sup>. However mitochondrial distress was only observed with the charged AuNPs. While the charged AuNPs induced both an increase in caspase-3 expression and nuclear localization of p53, the neutral AuNP showed an increase in p53 localization (nucleus and cytoplasm) only<sup>227</sup>. Thus the biological response is dependent on the surface properties of AuNPs: the charged AuNPs induce apoptosis and the neutral AuNP promote necrosis<sup>227</sup>. Likewise, the Rotello group also discussed the cytotoxicity of 2 nm cationic AuNPs with various hydrophobicity in HeLa cells using mitochondrial, ROS, and comet assays (measures DNA damage)<sup>228</sup>. The experimental outcome strongly suggests that the higher the hydrophobicity, the greater the observed acute toxicity and decreased DNA damage. Noticeably, these AuNPs can produce considerable amounts of reactive oxygen species (ROS) that oxidatively damage DNA at doses that do not affect mitochondrial activity<sup>228</sup>. The above studies show that the surface size as well as the charge of the nanoparticle plays a significant role in cytotoxicity and genotoxicity. These are important factors to keep in mind when designing nanomaterials for medicinal use.

In contrast, there are several studies that discuss the cytotoxic effects of silver nanoparticles. In an initial report by Hussain and coworkers, the toxic effects of AgNPs (15, 100 nm; [5 – 50  $\mu$ l]) were evaluated in rat liver cells (BRL 3A)<sup>229</sup>. After a 24-hour exposure, there was a significant decrease in mitochondrial function and LDH leakage. It was further hypothesized that AgNP toxicity is mediated via oxidative stress (increase in ROS, decrease in GSH, etc)<sup>229</sup>. A following study by Park *et al.* used RAW264.7 cells to elucidate the mechanism of AgNP toxicity<sup>230</sup>. The researchers exposed the RAW264.7 (exposure time; 24, 48, 72, and 96 h to) to 69 nm AgNPs with varying concentrations (0.2, 0.4, 0.8, and 1.6 ppm)<sup>230</sup>. Their results showed that the viability of the macrophages decreased in a dose and time dependent manner. Further cellular analysis revealed a dramatic decrease in GSH levels, a considerable increase in NO production and TNF- $\alpha$  (2.8-fold) along with a complete arrest at the G<sub>1</sub> phase of the cell cycle. Work by Piao *et al.* further clarified the mechanism of cytotoxicity of AgNPs (compared to AgNO<sub>3</sub>) using human Chang liver cells<sup>231</sup>. As shown in the previous studies, GSH levels were decreased while ROS levels increased in a time and concentration dependent manner when the cells were incubated with AgNPs. The researchers further elucidated that AgNPs modulate the expression of Bax and Bcl-2 (mitochondrial dependent apoptotic pathway) creating a loss of mitochondrial membrane potential (MMP)<sup>231</sup>. The subsequent release of cytochrome C (due to decrease in MMP) resulted in activating caspases-3 and -9 mediated by the JNK pathway. A more recent report by Teodoro *et al* not only corroborated the aforementioned deleterious effects of AgNPs; they also clearly demonstrate that silver nanoparticles contribute to cellular damage<sup>232</sup>. In that investigation the bioenergetics of rat liver mitochondria was evaluated after acute exposure to AgNPs (40 and 80 nm). Both sizes of AgNPs created an increase of the permeability of the inner mitochondrial membrane and subsequently leading to mitochondrial depolarization. This impairment of mitochondrial function resulted in an uncoupling effect on the oxidative phosphorylation system<sup>232</sup>. The molecular mechanism of AgNPs cytotoxicity was further defined in a very recent report by the Hyuan group<sup>233</sup>. Silver nanoparticles (ca. 40 nm) were incubated with both liver cells (human Chang liver) and Chinese hamster lung fibroblasts (V79-4) for up to 24 hrs with various concentrations. Using flow cytometry and confocal microscopy, exposure of AgNPs induced an overloading of mitochondrial Ca<sup>2+</sup> and enhanced ER stress<sup>233</sup>. Further analysis via Western blotting showed AgNPs increased the phosphorylation of PERK and IRE1 along with an up-regulation of GRP78/Bip, which are significant markers of ER stress. Altogether these results indicate that AgNPs induce ER stress that eventually leads to cellular apoptosis<sup>233</sup>. More importantly, this study also demonstrated AgNP cytotoxicity was not cell line

dependent<sup>233</sup>. The biological effects of AgNPs were also investigated using coronary endothelial cells (CECs) and aortic rings isolated from rats<sup>234</sup>. It was demonstrated that AgNPs induce NO-dependent proliferation in a dose and size dependent manner in CECs. Interestingly, at low concentrations AgNPs induced vasoconstriction in rat aortic rings but vasodilation at high concentrations. Thus the biological responses mediated by AgNPs are selective and specifically associated with the size and concentration of AgNPs.

The vast majority of toxicity studies performed is based on determining the proper dosage of nanoparticles. Despite the fact that “proper dosages” does not generate a “toxic response”, nanoparticles might modify cellular processes such as signal transduction<sup>235</sup>. For example, silver nanoparticles were shown to directly interact with Fyn kinase, thus creating signal interference in stem cells<sup>236</sup>. Likewise, cells treated with a low dose of nanoparticles were shown to reduce the activity of caspases<sup>237</sup>. In a recent experiment, researchers studied three of the most utilized nanomaterials (silver, gold, and iron; d= 10 nm) to determine the downstream effect normal cellular processes<sup>238</sup>. Human epithelial cell lines (A-431) were treated with 15  $\mu\text{g}/\text{mL}$  of metallic nanoparticles (of similar size and morphology) and the subsequent effect of the particles on EGF signal transduction was evaluated. As predicted, silver nanoparticles caused a substantial increase in ROS over either gold or iron particles. Gold nanoparticles had a considerable effect on EGF-dependent phosphorylation (20%), though the other particles also reduced phosphorylation levels to varying degrees. Iron nanoparticles had the greatest impact on EGF-dependent gene transcription; minimal alterations were seen with either gold or silver particles. The results of this in depth study demonstrate that metallic nanoparticles can disrupt cellular functionality, with the composition of the core material uniquely affecting the signaling response playing a significant role. The studies discussed above imply that care is needed in the use of nanoparticles in medicine. However with proper design, these studies also indicate the potential utility of these systems as cytotoxic therapeutic agents for cancer therapy.

#### 4.2 Effect of mode of administration

It is essential to have a firm understanding of how nanoparticles interact in biological systems *in vivo* if they are to be an effective pharmaceutical. Thus it is necessary to have proper characterization of these nanomaterials using the appropriate animal model alongside vigorous statistical analysis. Depending upon the route of administration, the pharmacokinetics, biodistribution, and toxicity profile of nanoparticles vary. For instance, a few studies demonstrate that intramuscular and intravenous injections of gold have a relatively higher uptake versus oral administration<sup>239, 240</sup>. As a case in point, the toxicity and pharmacokinetics profile of Auranofin (clinically approved gold complex drug-see Fig. 2) and gold sodium thiomalate (also a gold complex – see Fig. 2c) are well documented, nevertheless the mode of administration is still an on going debate<sup>241</sup>. While, the bioavailability of injected gold showed absorption maximum of only 20–25% after 2 h, intermittent dosing of gold resulted in erratic concentration levels within patients<sup>239, 242–244</sup>. Intravenous injection of gold complexes can also lead to some accumulation in the dermis and deposition in the cornea compared to oral administration<sup>245, 246</sup>. In contrast, orally administered gold complexes showed a higher half-life and a steady blood plasma concentration of throughout the treatment. Furthermore, the majority (85–95%) of the gold complex administered orally is excreted. However, the remaining amount (5–15%) is passed through the urine<sup>244, 247</sup>. The Brandau group compared the biodistribution of AuNPs (d= 1.4nm and 18 nm) using two routes of administration: (i) intratracheal instillation into the lungs (IT); and (ii) tail vein injections (IV)<sup>248</sup>. Analysis of the results indicated the smaller nanoparticle translocated through the respiratory tract after IT administration, whereas the 18 nm particle remained in the lungs<sup>248</sup>. After IV administration, both nanoparticles accumulated in the liver with the 18 nm AuNP showing 2-fold increase comparatively (18

nm =93.6% ID/g).. Work done in the Zhang group reported the toxicological features of 13.5 nm AuNP is also dependent on the route of administration<sup>249</sup>. A dose window of 137.5–2200 µg/kg was administered orally, intraperitoneal (IP), or in the tail vein injection of mice. The body weight, blood profile and other phenotypical changes of the mice was observed and recorded<sup>249</sup>. Injections via tail vein had minimal toxic effects showing minimal alterations to white blood cells and platelet counts. Additionally, the change of hemoglobin concentration was not statistically significant. However, intraperitoneal and oral administration showed increased toxicity with a reduction in red blood cell count<sup>249</sup>.

A recently reported study compared the biodistribution of silver salts (AgAc) to 14 nm PVP coated silver nanoparticles orally administered to rats<sup>250</sup>. Despite the formulation, the pattern of silver distribution into the organs was similar, with the highest concentrations found in the small intestine, stomach, kidneys, and liver though the uptake of silver in the kidney, liver, lung and other organs were quite lower for AgNP treatment with respect to AgAc treatment<sup>250</sup>. The excretion of silver for AgNP treatment was relatively high in fecal matter (63 %) than in urine (0.005 %). The amount of silver present in bile fluid was 16 to 20 fold greater than in rat plasma. Authometalliographic staining (AMG) showed silver only on the surface of intestinal (ileum) villi but not in the cellular cytoplasm. Renal papilla showed heavy staining of AMG grains in the glomeruli and renal tubules; Still, there was no change in the staining pattern between animals exposed to AgAc or AgNP<sup>250</sup>. Chrastina and Schnitzer reported the biodistribution of PVP coated and radio I<sup>125</sup> labeled AgNP (12 nm) in Balb/c mice injected intravenously<sup>251</sup>. The CT-SPECT (single photon emission computerized tomography) imaging revealed particles were mostly taken up by reticuloendothelial system (spleen 41.5 % and liver 24.5%) after 24 h; the rest were distributed in all other organs in very low amount. This indicates the particles relocate from the primary injection site and then further distributed to a secondary location<sup>251</sup>. However other reports indicate enhanced liver enzyme activity, higher uptake by local macrophages, increased inflammatory response, and liver damage<sup>251</sup>. This in depth analysis plainly demonstrated nanosilver toxicity is contingent on the route of administration. In addition, the toxic effects of silver nanoparticles are dose and time dependent.

It is worth briefly discussing the effect inhalation of nanoparticles may have on biological systems. Evidence of silver nanoparticle toxicity via inhalation was described in the *in vivo* studies performed by Sung *et al.* and Kim *et al.* using Sprague-Dawley rats. In the initial studies by Sung *et al.* investigated the possible biological effects of prolonged exposure to 18 nm AgNPs<sup>252</sup>. In this 90-day study, female and male rats were exposed AgNPs for 6 h/day, 5 days/week, for 13 weeks in a whole-body inhalation chamber. The end results of this study show that AgNPs reduce lung function and produce inflammatory lesions in the lungs in at a much lower mass dose concentrations ( $2.9 \times 10^6$  particles/cm<sup>3</sup>) compared to submicrometer particles. In their follow up study, bile-duct hyperplasia in the liver increased dose dependently in both the male and female rats under similar experimental conditions was observed<sup>253</sup>. In their most recent report rats were exposed to 18 nm AgNPs for 4 hours in a whole-body inhalation chamber and then further observed for 2 weeks. After a full analysis of lung function, the results demonstrated that acute inhalation exposure to silver nanoparticles may not cause acute toxicity<sup>254</sup>.

The results of the aforementioned studies was comparable to investigations by Kim *et al.* using 60 nm AgNPs stabilized with carboxymethylcellulose<sup>255</sup>. In this study, the effects of orally dosed AgNP (60 nm; dosimetry 30 mg/kg, 300 mg/kg and 1000 mg/kg) in both male and female rats was extensively monitored for 28 days<sup>255</sup>. Over the course of AgNP treatments, the rats did not show a significant change in body mass index regardless of their sex or dosage. However, blood chemistry analysis indicated elevated liver damage in the group with the medium dosage (300 mg/Kg) indicated by changes in ALP and cholesterol in

both male and female rats<sup>255</sup>. In a follow up study, 5 week old male and female rats were administered 56 nm AgNPs via subchronic inhalation (30 mg/kg, 125 mg/kg, 500 mg/kg) over a period of 90 days (13 weeks)<sup>256</sup>. Numerous other parameters such as metal ion ( $Mg^{+2}$ ,  $Na^{+}$ ,  $K^{+}$ ), total protein (albumin, gamma glutamyl transpeptidase, alanine aminotransferase, etc), reticulocyte, bilirubin, glucose, triglycerides, salt, calcium, blood counts, histology and ICP-MS analysis were done 90 days post treatment in both the male and female rats for all doses<sup>255</sup>. The mice with the lowest dosage (30 mg/kg) had no remarkable toxicity whereas with the 125-mg/kg dosages there was a noticeable effect. The body mass index was significantly decreased for male rats with the highest dosage (500 mg/kg) just after 4 weeks<sup>255</sup>. Histopathological analysis revealed considerable liver damage, through bile-duct hyperplasia, in both male and female rats and also a substantial change in cholesterol and ALP (alkaline phosphatase concentration) with the 125mg/kg dosage<sup>256</sup>. The concentration of silver of all the tissue samples collected showed a dose-dependent increase. Furthermore female rats had a 2-fold higher concentration of silver in the liver compared to the males. In conclusion, the above studies demonstrate that reduction in lung function and inflammatory lesions appear after AgNPs enter the body. Thus accumulation and, in some cases, damage tissues such as the liver, lungs, and olfactory bulbs, or penetrate the blood–brain barrier occurs.

#### 4.3 Effect of particle size and morphology

The physiochemical parameters such as charge, size, and shape of nanoparticles as well as the nature of the binding ligand have to be considered during nanoformulation in order to minimize toxicity and increase the therapeutic index. Initial work by Hillyer demonstrated that the distribution of AuNPs orally dosed was inversely proportional to the size of the nanoparticles. An investigation by Geertsma exemplified the wide dispersal of 10 nm gold nanoparticles throughout the body, while the larger particles were only observed in the liver, blood and spleen<sup>257</sup>. In another study by Pan et al, nanoparticles with a diameter of 1–2 nm are very toxic whereas 15 nm gold particles are relatively nontoxic in any cell type<sup>258</sup>. Furthermore, the authors showed that the cellular response is size dependent, even with particles of similar size. Abdelhalim et al. reported that Wistar-Kyoto rats infused with 10, 20 and 50 nm AuNP by a dosimetry of 3 or 7 days showed hepatotoxicity and renal toxicity<sup>259</sup>. The smaller size particles had more toxic effect than larger particles with ROS generation leading to necrosis, renal tubular alterations, higher Kupffer cell hyperplasia, and central veins intima disruption<sup>259</sup>. In a ground breaking study by Chen et al reported on the *in vivo* effect of naked particles ranging from 3 to 100 nm injected IP<sup>260</sup>. BALB/C mice were injected with the variant gold nanoparticles (8 mg/kg/week dose). It was found that 8 to 37 nm particles caused acute toxicity including loss of appetite, fur color change, sickness, reduced body weight, crooked spine (after 14 days) in contrast to normal mice (Fig. 11). However, particle core size of 3, 5, 50, 100 nm did not show any apparent toxicity. Histopathological analysis evidenced an increased population of Kupffer cell in hepatocytes and structural deterioration of the lungs, liver and spleen. These observations were linked to the presence of gold particles these sites, which were detected by AuNP enhanced CARS signal (Coherence anti-Stokes Raman Signal) (Fig. 12).

Ligands like mPEG, chitoan, dextran, polylactico glycolic acid (PLGA) can be functionalized onto the nanoparticle surface in order to improve blood retention time, decrease deposition into the liver and reduce immunogenic reactions. The pharmacokinetics and passive uptake of mPEG AuNPs of various size, (from 20 nm to 100 nm), into tumors was studied in tumor bearing CD1 mice<sup>261</sup>. The half-life of the smaller particles ( $t/2 = 51h$ ) was 8-fold higher compared to the larger particles ( $t/2 = 6.6 h$ ). Interestingly, the larger nanoparticles had a greater accumulation into the tumors, implying passive uptake into the matrix is core size dependent. The pharmacokinetics and biodistribution of PEG-AuNPs ( $d =$

20, 40, and 80 nm) were also examined in nude mice<sup>221</sup>. This investigation revealed that 20 nm AuNP had the longest half-life and significantly higher tumor extravasation compared with the 40 and 80 nm AuNPs.

Park et al reported the size dependent toxicity of the silver nanoparticle when mice were exposed to 1mg/kg of AgNP (22, 42, 71, 323 nm) by oral dosage for two weeks<sup>262</sup>. The 22 nm particles showed increased toxicity with higher immune cell infiltration (B cell & higher CD8+ T cell subtypes) and increased level of TGF- $\beta$  and cytokine production (specially IL-10 and 12) whereas the larger size particles did not have an adverse effect (Fig. 13). The organ weight was unaltered in any of these treatments irrespective of size as compared to controls<sup>262</sup>. The 22 nm particles count was higher in brain tissue (possibly penetrating blood-brain barrier) than larger particles, which were not well distributed in the brain. There was also a dose dependent toxicity (0.25 mg/kg, 0.5 mg/kg and 1.0 mg/kg) for 42 nm particles with the highest treatment dosage showing an increase in ALP, AST (aspartate transaminase), and ALT (alanine transaminase) levels. Histopathology analysis indicated minor damage to the cortex of the kidneys, but serious changes in morphology in the liver and small intestines was not noted<sup>262</sup>. In a analogous study by the De Jong group, the authors demonstrated a size dependent (20, 80 and 110 nm) biodistribution of silver nanoparticles via IV administration for 5 consecutive days and further monitored for 16 days<sup>263</sup>. Nanoparticles were rapidly cleared from circulation and dispersed to all the organs irrespective of size. Larger particles mostly accumulated in spleen, followed by the liver and lung, while small particles (20 nm) were primarily deposited in the liver, then subsequently distributed to the kidneys and spleen<sup>263</sup>.

Nanomaterials undergo aggregation upon contact with biological fluid and media, thus changing their identity and possible effects on living systems<sup>134</sup>. Gosens elegantly demonstrated the effects of individual nanoparticles (50 and 250 nm) and their aggregates by using a pulmonary inflammation animal model in male rats<sup>264</sup>. The study of pulmonary inflammatory markers (cytokines), TEM analysis, cell counts and cytotoxicity analysis from bronchoalveolar lavage fluid (BALF) indicated that citrate coated 50 nm and 250 nm (single particles) as well as their aggregates did not cause severe toxicity, with the exception of mild pulmonary inflammation. Additional analysis of blood cell counts (lymphocytes, basophils, neutrophils, eosinophils and macrophages), concentration of inflammatory cytokines (TNF- $\alpha$ , IL-6) and other serum protein (fibrinogen, LDH, albumin) level were unaltered in both single and agglomerated particles<sup>264</sup>.

#### 4.4 Effect of Surface Chemistry

The surface chemistry of nanoparticles is also an influential factor in pharmacokinetics and biodistribution. This information could provide design principles for optimizing delivery to tumors. For instance, in one study mice were injected with one of five types of gold nanoparticles ( $d = 5 - 22$  nm) containing either a positive, negative or neutral surface charge<sup>265</sup>. Analysis of the blood, excrement, and various tissues demonstrated that the positive 5 nm AuNP was higher in the blood post injection compared to the other charged nanoparticles. Additionally, the positive nanoparticle was also observed to have the largest accumulation in the kidneys (24% ID/g) and thusly “trapped”. The negative and neutral charged particles show statistically significant accumulation in the liver comparatively<sup>265</sup>. Biodistribution studies in different mouse strains (immunodeficient vs. immunocompetent) demonstrated that surface charge of gold nanoparticles and their modes of systemic administration uniquely alter their pharmacokinetics, organ distribution and tumor uptake<sup>266</sup>. Neutral and zwitterionic particles provide high systemic exposure and low clearance when administered through intravenous administration. Intraperitoneal-administered nanoparticles demonstrated substantially lower systemic exposure than the IV-administered nanoparticles, suggesting inability of the particles to cross the peritoneal

barrier. Low plasma clearance for both administration routes was reflected in the increased tumor uptake of the neutral and zwitterionic nanoparticles in a subcutaneously implanted xenograft model of ovarian cancer<sup>266</sup>. Furthermore, AuNPs administered IV accumulated mainly in the liver followed by the spleen and kidneys (positive AuNPs had the least accumulation), however IP administered AuNPs were concentrated in the pancreas, followed by the RES<sup>266</sup>. Particle size along with its surface charge can also mediate its biodistribution. In a study by Hirn and co-workers, rats were injected into the tail vein with radio labeled gold nanoparticles of various sizes (1.4–200 nm) and charges (positive or negative)<sup>267</sup>. The biodistribution of the negatively charged <sup>198</sup>-AuNPs was shown to be size dependent and had the greatest accumulation in the liver<sup>267</sup>. However the accumulation of the positively charged particles had a varied pattern. It was further hypothesized that protein binding and exchange on the particles surface modulated the uptake of the nanoparticles<sup>267</sup>. Finally, in a study by Zhu and coworkers, zebra fish were exposed to AuNPs (HD ≈ 10 nm) of various surface charge (hydrophilic: positive, negative, neutral, and a hydrophobic positive) over a range of times (24, 48 and 72 hours)<sup>268</sup>. Over time, it was shown that the positive nanoparticles were taken up more readily than the negative and neutral AuNPs. However, fish exposed to the hydrophobic AuNPs expired within 24 hours. The positive, negative and neutral AuNPs mostly accumulated in the intestine. Additionally, the charged AuNPs were excreted whilst the neutral AuNP tended to stay in the body. In contrast, the hydrophobic AuNP appeared to be more widely distributed with the largest concentration seen in the gills, heart and dorsal fin. These results are indicative of a strategic methodology: development of hydrophilic nanoparticles decreased their toxic profile.

#### 4.5 Accumulation of Nanoparticles in the Brain

Nanoparticle therapeutics is currently being developed to combat brain disorders such as Parkinson and Alzheimer's. In order to treat these diseases, nanoparticles must be able to cross the blood brain barrier (BBB) without harming the integrity of the brain. One investigation found that 24 hours after exposure, AgNPs and copper nanoparticles injected intravenously into rats resulted in edema localized to the proximal frontal cortex and the ventral surface of the brain<sup>269</sup>. Analogous findings were observed in mice that were systemically exposed to AgNPs or through a direct injection into the brain ventricular space<sup>270</sup>. In another investigation, inductively coupled plasma mass spectrometry (ICP-MS) and transmission electron microscopy was used to analyze the distribution of AgNPs (50–100 nm) in the main organs of rats<sup>271</sup>. After subcutaneous injection, the authors observed that AgNPs were mainly dispersed in the kidneys, liver, spleen, lungs, and brain as discrete nanoparticles<sup>271</sup>. These results were markedly different from another publication using BSA coated AgNPs 2 nm in size injected via IP<sup>272</sup>. Tissues were harvested from the rats after 24, 96, and 168h and assessed for silver content using ICP-MS and imaged using TEM. ICP analysis revealed significant accumulation of silver in the liver and spleen after 96 and 168 h exposure to AgNPs. Closer examination of brain tissue revealed evidence of silver induced damage even though AgNPs were not observed via TEM imaging<sup>272</sup>. It was further hypothesized by the authors that Ag can cross the blood brain barrier, but not as a defined nanoparticle<sup>272</sup>. In a report from the Soto group, 12.5 nm AuNPs (40, 200, 400 µg/kg/day) were administered to the tail vein of mice every day for 8 days. In all of the organs examined, there was a proportional increase in gold accumulation, including uptake into the brain. Their findings demonstrate the possibility of targeting brain tissue using AuNPs without generating noticeable toxicity<sup>273</sup>. In a contrasting report, AgNPs of various sizes (25, 40, 80 nm) were used to investigate their inflammatory effects on primary rat brain microvessel endothelial cells (rBMEC)<sup>274</sup>. Accumulation into the rBMECs was demonstrated to be size dependent, with the 25 nm AgNP showing the largest uptake. Furthermore the 25 nm AgNP also showed to have significant effect on cellular viability, permeability, cytotoxicity, morphology and inflammatory response as opposed to cells

exposed to the 40 and 80 nm AgNPs<sup>274</sup>. The results of these studies indicate more work needs to be done to produce a viable therapeutic nanoparticle for neurological diseases.

#### 4.6 Surface Permeation of Nanoparticles *in vivo*

The therapeutic applications of metallic nanoparticles are fairly diverse. With its touted antimicrobial properties, silver particles are found in a wide range of products ranging from clothing to topical creams. Even so, the safety profile for silver in these applications is still under investigation. Korani et al reported the dermal toxicity of silver nanoparticles in the animal model of male guinea pigs<sup>275</sup>. For the subchronic toxicity study, a concentration range of (100, 1000 and 10,000  $\mu\text{g/mL}$ ) nanosilver was selected whereas for acute measurement only two doses (1000 and 10,000  $\mu\text{g/ml}$ ) were chosen. For animals treated topically, a reduction in the thickness of the epidermis and dermis was observed in the low-dose group, with a slight increase of inflammatory Langerhans cells. However collagen fibers were reported to be normal. Skin toxicity was shown to be dose dependent; an increase in the concentration of AgNP manifested skin toxicity. During the course of the acute study, animals exposed to 10,000  $\mu\text{g/ml}$  of nanosilver had disrupted collagen fibers as well as a higher macrophage infiltration with acidophilic cytoplasm<sup>275</sup>. It was also observed that damage to hepatocytes (indicated with the higher amount of Kupffer cells) as well as some necrosis is also dose dependent, but spleen toxicity was not seen with histopathological analysis<sup>275</sup>. Using a porcine skin model, AgNPs were revealed to be in the upper stratum corneum layers of the skin<sup>276</sup>. Treatment with AgNPs caused localized inflammation (circa 14 days), whilst AgNPs cultured with keratinocytes were observed to be enclosed in cytoplasmic vacuoles<sup>276</sup>. After application to damaged human skin, transmission electron microscopy revealed silver penetration in the outermost layer of the epidermis and deep stratum corneum<sup>277</sup>.

Particle size was also shown to be a factor for *in vivo* permeation. Makino et al used citrate capped gold nanoparticles with different core sizes ( $d = 15, 100$  and  $200$  nm) and determined their permeation coefficient<sup>278</sup>. They demonstrated that the 15 nm AuNP had the greatest permeation, being found in the deep regions of the skin. However the larger particles remained on the surface of the skin<sup>278</sup>. In subsequent experiments, mice were injected with gold nanoparticles ( $d = 15, 50, 100$  and  $200$  nm) to study their ensuing biodistribution<sup>279</sup>. Analysis using inductively coupled plasma mass spectrometry (ICP-MS) revealed that most of the gold, regardless of size, was present in the liver, lung and spleen. The smallest nanoparticle displayed the greatest biodistribution throughout the mouse. Furthermore, both the 15 nm and 50 nm AuNPs crossed the blood brain barrier. However, the presence of the 200 nm particle was very insignificant in any of the tissues analyzed<sup>279</sup>.

#### 4.7 Effect on Embryonic Development

Beside mammals, other non-mammalian systems such as Zebra fish, *Drosophila* and *C. elegans* has also been used to evaluate the toxicity of silver nanoparticles<sup>280</sup>. Gorth *et al.* studied the effect silver nanoparticles had on the growth rate of *Drosophila*, from egg to pupate<sup>281</sup>. They found that smaller sized particles (20–30 nm) had mild effect on the growth rate. Eggs treated with larger particles showed significant toxicity (500–1200 nm) with only 10% developing to pupate at a 100-ppm concentration. The toxicity occurred via Hsp-70 upregulation, oxidative damage, and lipid peroxidation in the larvae<sup>281</sup>. The transport and biocompatibility of AgNPs was investigated using real time. In this study, Kim *et al.* used single AgNPs (5 – 46 nm) to determine the mechanism of transport in developing embryos<sup>282</sup>. The authors observed AgNPs accumulation throughout the development stage, with abnormal development relating to the concentration of AgNPs (Fig. 14)<sup>282</sup>. Another study using Zebra fish models, a dose dependent toxicity and phenotype changes were also observed. Treatment with silver nanoparticles resulted in abnormal phenotypic shapes such

as twisted body axes and notochord, as well as pericardial edema<sup>283</sup>. Beside that, hepatotoxicity and changes in mRNA level for several detoxifying enzymes like catalase, glutathione peroxidase were decreased whereas Bax, p21, Noxa genes were upregulated<sup>255, 283, 284</sup>. A similar report published by Wu *et al.* studied the early development of Japanese Medaka (*Oryzias latipes*). The authors observed fin fold malformations, oxidative DNA damage, and genetic aberrations<sup>285</sup>. Silver nanoparticles suspended in water can also exacerbate the hypoxic sensation of the Eurasian perch fish (*Perca fluviatilis*)<sup>286</sup> as well as severely affecting embryonic growth of oysters due to increased mRNA production of metallothionein<sup>287</sup>. Additional genomic analysis of *C. elegans* treated with AgNPs revealed the impairment of reproductive budding due to up-regulation of SOD-3 (superoxide dismutase) aberration in daf-12 genes<sup>280, 288</sup>. However, in a study by Browning *et al.*, they observed that AuNPs (11.6 nm) are much more biocompatible than AgNPs<sup>289</sup>. In their investigation, they observed AuNPs were able to passively diffuse through chorionic-pore-canals. Even though the amount of AuNPs accumulation was directly related to its concentration, the majority of the embryos (74%) developed into normal fish<sup>289</sup>.

#### 4.8 Other potential side effects of nanoparticles

Argyria is one of the reported side effects in patients exposed to colloidal silver. Over a long period of time, silver will deposit in the skin thus giving the patient a blue hue (via ingestion of 6.4 g of colloidal silver over a period of a year)<sup>290</sup>. Besides that, night vision problems, bowl pain, respiratory trouble, reduced creatinine clearance, increase in  $\beta$ -acetyl-B-D glucoseaminidase are also associated with the workers exposed to silver dust<sup>291, 292</sup>. Some of the workers also had tarnished corneas and conjunctiva due to inhalation<sup>293</sup>. Another report discusses a patient that ingested colloidal silver three times a year over a two-year period resulted in hyperlipidemia, diabetics and hypertension along with blue-grey facial color<sup>294</sup>. Other accounts of neurological disorders was recently documented in a 75 year old man who self mediated with colloidal silver<sup>295</sup>. Exposure to AgNPs via inhalation over a 14-day period can also stimulate the expression of 468 genes in the cerebrum. Amongst these, several genes were linked to numerous neurodegenerative disorders<sup>296</sup>. Rahman *et al.* demonstrated similar results of neurotoxicity from AgNPs. Analysis of mouse brains exposed to nanosilver yielded increased ROS generation, apoptosis and gene modulation<sup>297</sup>. The studies presented here yielded different results seen of patients with poisoning from silver inhalation. This clearly illustrates the need for more in-depth studies on the safety profiles of nanosilver prior to commercial use.

As mentioned earlier, gold collids has been used for centuries in medicine without any notable side effects. One contributing factor is largely due to the fact that gold (0) is extremely inert<sup>298</sup>. Gold is also used in small quantities in dental prostheses, pastries, chocolates and sometimes in alcoholic beverage<sup>181</sup>. Nonetheless, enzymes from saliva can transform gold (0) to gold (I), which is consequently engulfed by immune cells<sup>181, 299</sup>. By and large the observed toxicity for gold (I) compounds is skin and mucous hypersensitivity along with macular and papular rash, eosinophilia, erythema nodosum and various other allergic reactions<sup>300</sup>. In some cases, oral administration of gold complexes have also been reported to trigger diarrhea<sup>301</sup>. Very low incidence of nephrotoxicity has been reported with minor proteinuria while injected with gold complexes<sup>302, 303</sup>. Gold complexes can also generate some hematological disorders and is not recommended for pregnant women due to its teratogenic properties<sup>304</sup>. Other toxicological effects is due to the oxication of effects of gold (I) to gold (III) by phagolysosomal enzymes and other redox proteins such as myeloperoxidase<sup>181</sup>. The major cause of this toxicity has been attributed to free radical formation, thereby causing oxidative stress<sup>305</sup>. The slow clearance of these nanoparticles and their increasing accumulation in the liver and spleen, kidneys and lungs can also be the



cause of increased damage due to oxidation<sup>181</sup>. It has also been reported that nanoparticles trigger thrombosis, hemolysis and other immunogenic reactions while being systemically transported<sup>306</sup>.

In healthy conditions, the human body contains a basal level of gold in the range of 0–0.001 ppm<sup>307</sup>. Gold is also found in small amounts in skin (0.03 ug/g), hair (0.3 ug/g) and nails (0.17  $\mu\text{g/g}$ )<sup>239, 245, 247, 308</sup>. Gold (I), relatively inert compared to gold (III), is reasonably stabilized in aqueous solution via capping agents. Most of the gold in circulation gets adsorbed by albumin and/or globulin and remain bound to plasma for months<sup>309</sup>. Depending on the patient, systemic gold uptake is varied. For instance, with patients that are smokers, there is an increased adherence of gold to red blood cells<sup>239, 310</sup>. It is mostly absorbed in the lymphatic and reticuloendothelial systems (due to their metal absorbing capacity) whereas liver and bone marrow account for 25 % of the total uptake<sup>239, 242, 308</sup>.

#### 4.9 Toxic Effect of Other Metallic Nanoparticles

Some toxicological reports are also documented for other metal nanoparticles beside gold and silver metal<sup>311</sup>. In comparative study, Ashrarani *et al* reported on the size dependent toxicity of Au, Ag and platinum nanoparticles using zebrafish model over 72 hour period<sup>131</sup>. They found polyvinyl alcohol capped (PVP) Pt particles (3–10 nm) delayed hatching, impaired the mortality, crippled backbone, cardiac abnormality, along with brain accumulation of platinum. Gold and silver uptake was quite high compared to platinum as evidenced by ICP-OES. Yet, the toxic profile of gold nanoparticles was trivial relative to silver nanoparticles (highest toxic profile) and moderate for platinum particles<sup>131</sup>. Hussain *et al*. reported that manganese (Mn-40 nm) particles can trigger oxidative stress in neuroendocrine cells (PC-12) and a dose dependent cleavage of dopamine (DA) and its metabolite<sup>312</sup>. It is known that manganese has potential to cause *in vitro* and *in vivo* toxic effects, however not much is published on MnNP<sup>313</sup>. The experimental evidence with morphological assessment, MTT assay, and metabolite measurements of DA indicates the neurotoxicity of the MnNP<sup>312, 313</sup>. Another report by Wang *et al* demonstrated the neurotoxicity of manganese and copper nanoparticles in PC-12 cell lines<sup>314</sup>. Copper particles (90 nm) had similar effects as MnNPs such as DA depletion and modulation of gene expression. Monoamine oxidase A (maoa) was enhanced by Cu-90 nm treatment while tyrosine hydroxylase (Th) was down regulated by Mn-40 nm treatment<sup>314</sup>. There was no major effect observed for Ag-15 treated with MnNPs in relationship to dopamine regulation even at a high dose. Many ROS responsive genes (gpx1, gss) and neuro pathophysiological relevant genes (park2,  $\alpha$ -synuclein) were also altered by the Cu-90 nm and Mn-40 nm treatment<sup>314</sup>. This is indicative of oxidative stress mediated by dopamine degradation. Both Mn-40 nm and Cu-90 nm treatment caused upregulation of Snca and Park2. Both proteins are often linked with many neurodegenerative diseases such as Parkinson's and Alzheimer due to proteins being generated with an aberrant confirmation<sup>314</sup>. These studies implicate that CuNP and MnNP particle mediated protein misfolding can lead to neurotoxicity and neurological pathogenesis in dopaminergic cells, having a susceptibility to cross the blood brain barrier (BBB)<sup>314</sup>. Prabhu *et al* reported a dose (10–100  $\mu\text{M}$ ) and size dependent toxicity of Cu-NP (40, 60, 80 nm) treated for 24 h in a dorsal root ganglion (DRG) cell derived model from rats<sup>315</sup>. Cell viability study (MTT assay) and light microscopic analysis indicated the formation of vacuoles and neurons depletion and neurite network cleavage<sup>315</sup>. The Cu particle showed maximum toxicity at highest dose and smaller size. The effect of Cu-NP toxicity could occur due to disruption of mitochondrial dehydrogenase activity *in vitro* and *in vitro*, thus triggering ROS production. Chen *et al* reported that oral dosage (LD<sub>50</sub> 413mg/kg) of copper nanoparticles in mice might cause severe toxicity to many organs such as kidney, liver, spleen, brain<sup>316</sup>. The *in vitro* analysis showed the gerneation of Cu<sup>3+</sup> ion is the cause of lethality, which could have a different *in vivo* metabolism<sup>317</sup>.

Furthermore copper nanoparticle can be smoothly absorbed into body through skin and respiratory tract. Given the increasing use and demand of nanomaterials in industry, healthcare, and cosmetics, safety measures are a necessity to protect human health and the surrounding environment.

## 5. Concluding remarks and Future outlook

In this review, we have discussed modern synthesis and some recent applications of noble metal nanoparticles in medicine. We have also described some possible toxic affect these particles may elicit on living systems and their surrounding environment. One of the major challenges in nanobiotechnology is to improve the efficacy of nanoparticle therapeutic and the reduction of any intrinsic side effect. With the rapid surge in the development in nanomaterials, new treatment strategies are being explored that has the potential to overcome existing problems using noble metal nanoparticles. Even with their fantastic promise, the impact on human health (postive and negative) needs to be fully understood prior to wide spread use. Furthermore, our experimental setups need to be well thought out and carefully executed for proper interpretation of the data presented. In a recent publication, it was eluded that the uptake and subsequent affects nanoparticles elicit on cells might be arbitrary<sup>318</sup>. The cellular uptake of nanoparticles is paramount to their therapeutic applications and possible toxicity. Thus when designing *in vitro* experiments, numerous other aspects must be considered. As mentioned earlier, nanoparticles may aggregate in biological medium<sup>134</sup>, due to the high ionic environment, and settle. This sedimentation might effect the dynamic interactions between the nanoparticles and the cells. Furthermore, the authors argue the probability that the uptake of nanoparticles and subsequent cellular response is variable. Other considerations also need to be made when conducting *in vitro* experiments such as the protein corona. When nanoparticles are exposed to biological fluids, they may interact and be coated with proteins in solution. This protein coating, or protein corona, mediates the biological response and the intrinsic physical-chemical properties of the nanoparticle<sup>126</sup>. These factors mentioned above should be taken into careful consideration when designing the experimental setup, executing the plan, and in data interpretation.

For a successful translation of nanoparticles to the clinics, several features need to be considered. First of all, the attributes and characteristics of nanoparticle therapeutics need to be strictly and rigorously defined. Throughout the literature, it is apparent that the biodistribution and pharmacokinetics is largely dependent on the nanomaterial. Thus necessary measures need to be done to examine possible toxic effects of each nanoparticle fabricated. Even though there are several reports stating “naked” gold nanoparticles are biologically inert (evident since its medicinal use in antiquity), the capping agents may change the toxic profile of the particle. Similarly, the hydrodynamic diameter and surface charge may also affect the efficacy of the nanoparticle. The increasing surface size as well as charge modulation affects the cell-nanoparticle dynamics<sup>32, 140, 170</sup>. Furthermore, the increase in hydrophobicity of the nanoparticle surface is directly related to the toxic effect in living systems<sup>268</sup>.

The application of nanoparticles in medicine is an emerging field with the potential to have a positive effect on human healthcare. Although more research is necessary, nanotechnology can play an intimate role in individualized medicine. Since they show fundamentally new properties at the atomic and supramolecular scales (1 100 nm), novel molecular architectures can be fabricated with a high degree of precision and flexibility. Owing to these intrinsic properties, noble metal nanoparticles can be fine-tuned to be effective therapeutics and diagnostic agents.

## References

1. Norton S. *Mol Interv.* 2008; 8:120–123. [PubMed: 18693188]
2. Thompson, C. *Alchemy and Alchemists*. Dover Publications, Inc; Mineola, NY: 2002.
3. Grene, D. *Herodotus The History*. University of Chicago Press; Chicago: 1987.
4. Higby GJ. *Gold Bulletin.* 1982; 15:130–140. [PubMed: 11614517]
5. Kauffman G. *Gold Bulletin.* 1985; 18:69–78.
6. Koch, R. *On bacteriological research*. Hirsch Forest; Berlin: Aug. 1890
7. Forestier J. *The Lancet.* 1934; 224:646–648.
8. Shaw CF. *Chemical Reviews.* 1999; 99:2589–2600. [PubMed: 11749494]
9. Hammond, CR. *The Elements*. CRC Press; Boca Raton, FL: 2000.
10. Magner, LN. *A History of Medicine. 2*. Informa Healthcare; New York, NY: 1992.
11. Atiyeh BS, Costagliola M, Hayek SN, Dibo SA. *Burns.* 2007; 33:139–148. [PubMed: 17137719]
12. Dunn P. *Arch Dis Child Fetal Neonatal Ed.* 2000; 83:158–159.
13. Garrett TP. *The Art World.* 1917; 2:489–491.
14. Wood, I. *Platinum*. Benchmark Books; New York: 2004.
15. Benner, LS.; Suzuki, T.; Meguro, K.; Tanaka, S. *Precious Metals: Science and Technology*. IPMI Press; Allentown, PA: 1991.
16. Rosenberg BV, Krigas LT. *Nature.* 1965; 205:698–699. [PubMed: 14287410]
17. Rosenberg BV, Grimley L, Thomson E, AJ. *J Bio Chem.* 1966; 242:1347–1352. [PubMed: 5337590]
18. Trzaska S. *C&EN News.* 2005; 83:3.
19. Perks B. *Chemistry World.* 2010 Sep.:48–50.
20. Brown C, Bushnell G, Whitehouse M, Agarwal D, Tupe S, Paknikar KM, Tiekink E. *Gold Bulletin.* 2007; 40:245–250.
21. Barber DJ, Freestone IC. *Archaeometry.* 1990; 32:33–45.
22. Mody VV, Siwale R, Singh A, Mody HR. *J Pharm Bioallied Sci.* 2010; 2:282–289. [PubMed: 21180459]
23. Padovani S, Sada C, Mazzoldi P, Brunetti B, Borgia I, Sgamellotti A, Giulivi A, D'Acapito F, Battaglin G. *J Appl Phys.* 2003; 93(10058):93.
24. Faraday M. *Philosophical Transactions of the Royal Society of London.* 1857; 147:145–181.
25. Mle G. *Annalen der Physik.* 1908; 25:377–445.
26. Feynman R. *Resonance.* 2011; 16:890–905.
27. McDonald D. *Platinum Metals Rev.* 1965; 9:136–139.
28. Dayanand SA, Shreedhar B, Dastager SG. *Digest Journal of Nanomaterials and Biostructures.* 2010; 5:447–451.
29. Bonini M, Lenz S, Giorgi R, Baglioni P. *Langmuir.* 2007; 23:8681–8685. [PubMed: 17625901]
30. Giljohann DA, Seferos DS, Daniel WL, Massich MD, Patel PC, Mirkin CA. *Angewandte Chemie International Edition.* 2010; 49:3280–3294.
31. Hayat, M. *Colloidal Gold Principles, Methods and Applications*. Academic Press; San Diego, London: 1989.
32. Khan JA, Kudgus RA, Szabolcs A, Dutta S, Wang E, Cao S, Curran GL, Shah V, Curley S, Mukhopadhyay D, Robertson JD, Bhattacharya R, Mukherjee P. *PLoS ONE.* 2011; 6:e20347. [PubMed: 21738572]
33. Turkevich J, Stevenson PC, Hillier J. *Discussions of the Faraday Society.* 1951; 11:55–75.
34. Frens G. *Nature: Phys Sci.* 1973; 241:20.
35. Ji X, Song X, Li J, Bai Y, Yang W, Peng X. *Journal of the American Chemical Society.* 2007; 129:13939–13948. [PubMed: 17948996]
36. Ojea-Jimenez I, Romero FM, Bastus NG, Puntès V. *The Journal of Physical Chemistry C.* 2010; 114:1800–1804.
37. Bastus NG, Comenge J, Puntès V. *Langmuir.* 2011; 27:11098–11105. [PubMed: 21728302]

38. Schmid G. *Chemical Reviews*. 1992; 92:1709–1727.
39. Giersig M, Mulvaney P. *Langmuir*. 1993; 9:3408–3413.
40. Brust M, Walker M, Bethell D, Schiffrin DJ, Whyman R. *Journal of the Chemical Society, Chemical Communications*. 1994:801–802.
41. Daniel M-C, Astruc D. *Chemical Reviews*. 2003; 104:293–346. [PubMed: 14719978]
42. Schaaff TG, Knight G, Shafiqullin MN, Borkman RF, Whetten RL. *The Journal of Physical Chemistry B*. 1998; 102:10643–10646.
43. Schaaff TG, Whetten RL. *The Journal of Physical Chemistry B*. 1999; 103:9394–9396.
44. Whetten RL, Khoury JT, Alvarez MM, Murthy S, Vezmar I, Wang ZL, Stephens PW, Cleveland CL, Luedtke WD, Landman U. *Advanced Materials*. 1996; 8:428–433.
45. Prasad BLV, Stoeva SI, Sorensen CM, Klabunde KJ. *Langmuir*. 2002; 18:7515–7520.
46. Hicks JF, Miles DT, Murray RW. *Journal of the American Chemical Society*. 2002; 124:13322–13328. [PubMed: 12405861]
47. Ackerson CJ, Jadzinsky PD, Sexton JZ, Bushnell DA, Kornberg RD. *Bioconjugate Chemistry*. 2010; 21:214–218. [PubMed: 20099843]
48. Dharmaratne AC, Krick T, Dass A. *Journal of the American Chemical Society*. 2009; 131:13604–13605. [PubMed: 19725520]
49. Donkers RL, Lee D, Murray RW. *Langmuir*. 2004; 20:1945–1952.
50. Jadzinsky PD, Calero G, Ackerson CJ, Bushnell DA, Kornberg RD. *Science*. 2007; 318:430–433. [PubMed: 17947577]
51. Negishi Y, Nobusada K, Tsukuda T. *Journal of the American Chemical Society*. 2005; 127:5261–5270. [PubMed: 15810862]
52. Negishi Y, Takasugi Y, Sato S, Yao H, Kimura K, Tsukuda T. *Journal of the American Chemical Society*. 2004; 126:6518–6519. [PubMed: 15161256]
53. Parker JF, Weaver JEF, McCallum F, Fields-Zinna CA, Murray RW. *Langmuir*. 2010; 26:13650–13654. [PubMed: 20695616]
54. Reilly SM, Krick T, Dass A. *The Journal of Physical Chemistry C*. 2009; 114:741–745.
55. Wu Z, Suhan J, Jin R. *Journal of Materials Chemistry*. 2009; 19:622–626.
56. Parker JF, Fields-Zinna CA, Murray RW. *Accounts of Chemical Research*. 2010; 43:1289–1296. [PubMed: 20597498]
57. Brown KR, Walter DG, Natan MJ. *Chemistry of Materials*. 1999; 12:306–313.
58. Skrabalak SE, Xia Y. *ACS Nano*. 2009; 3:10–15. [PubMed: 19206242]
59. Frattini A, Pellegrini N, Nicastro D, Sanctis Od. *Materials Chemistry and Physics*. 2005; 94:148–152.
60. Bonsak J, Mayandi J, Thøgersen A, Stensrud Marstein E, Mahalingam U. *physica status solidi (c)*. 2011; 8:924–927.
61. Evanoff DD, Chumanov G. *Chemphyschem*. 2005; 6:1221–1231. [PubMed: 15942971]
62. Lee PC, Meisel D. *The Journal of Physical Chemistry*. 1982; 86:3391–3395.
63. Tao A, Sinsermsuksakul P, Yang P. *Angewandte Chemie*. 2006; 118:4713–4717.
64. Creighton JA, Blatchford CG, Albrecht MG. *Journal of the Chemical Society, Faraday Transactions 2: Molecular and Chemical Physics*. 1979; 75:790–798.
65. Dong X, Ji X, Wu H, Zhao L, Li J, Yang W. *The Journal of Physical Chemistry C*. 2009; 113:6573–6576.
66. Kvitek L, Prucek R, Panacek A, Novotny R, Hrbac J, Zboril R. *Journal of Materials Chemistry*. 2005; 15:1099–1105.
67. Panáček A, Kvítek L, Prucek R, Kolář M, Veceřová R, Pizúrová N, Sharma VK, Nevěčná Tj, Zbořil R. *The Journal of Physical Chemistry B*. 2006; 110:16248–16253. [PubMed: 16913750]
68. Yin Y, Li Z-Y, Zhong Z, Gates B, Xia Y, Venkateswaran S. *Journal of Materials Chemistry*. 2002; 12:522–527.
69. Panáček A, Kvitek L, Prucek R, Kolar M, Veceřová R, Pizúrová N, Sharma VK, Nevěčná Tj, Zbořil R. *The Journal of Physical Chemistry B*. 2006; 110:16248–16253. [PubMed: 16913750]
70. Barnes KR, Lippard SJ. *Metal ions in biological systems*. 2004; 42:143–177. [PubMed: 15206102]

71. Herricks T, Chen J, Xia Y. *Nano Letters*. 2004; 4:2367–2371.
72. Eklund SE, Cliffler DE. *Langmuir*. 2004; 20:6012–6018. [PubMed: 16459624]
73. Guo JW, Zhao TS, Prabhuram J, Wong CW. *Electrochimica Acta*. 2005; 50:1973–1983.
74. Gehrke H, Pelka J, Hartinger C, Blank H, Bleimund F, Schneider R, Gerthsen D, Brase S, Crone M, Turk M, Marko D. *Archives of Toxicology*. 2010; 85:799–812. [PubMed: 21229235]
75. Ahmadi TS, Wang ZL, Green TC, Henglein A, El-Sayed MA. *Science*. 1996; 272:1924–1925. [PubMed: 8662492]
76. Teow Y, Valiyaveetil S. *Nanoscale*. 2010; 2:2607–2613. [PubMed: 20936240]
77. Bratlie KM, Lee H, Komvopoulos K, Yang P, Somorjai GA. *Nano Letters*. 2007; 7:3097–3101. [PubMed: 17877408]
78. Bigall NC, Härtling T, Klose M, Simon P, Eng LM, Eychmüller A. *Nano Letters*. 2008; 8:4588–4592. [PubMed: 19367978]
79. Abid JP, Wark AW, Brevet PF, Girault HH. *Chemical Communications*. 2002:792–793. [PubMed: 12119726]
80. Eustis S, Krylova G, Eremenko A, Smirnova N, Schill AW, El-Sayed M. *Photochemical & Photobiological Sciences*. 2005; 4:154–159. [PubMed: 15616707]
81. Sudeep PK, Kamat PV. *Chemistry of Materials*. 2005; 17:5404–5410.
82. Hu B, Wang S-B, Wang K, Zhang M, Yu S-H. *The Journal of Physical Chemistry C*. 2008; 112:11169–11174.
83. Pyatenko A, Yamaguchi M, Suzuk Mi. *J Phys Chem C*. 2007; 111:7910–7917.
84. Eustis S, Hsu H-Y, El-Sayed MA. *The Journal of Physical Chemistry B*. 2005; 109:4811–4815. [PubMed: 16863133]
85. Eustis S, El-Sayed MA. *The Journal of Physical Chemistry B*. 2006; 110:14014–14019. [PubMed: 16854091]
86. Sau TK, Pal A, Jana NR, Wang ZL, Pal T. 2001; 3:257–261.
87. Kabashin AV, Meunier M. *Journal of Applied Physics*. 2003; 94:7941.
88. Tarasenko NV, Butsen AV, Nevar EA, Savastenko NA. *Applied Surface Science*. 2006; 252:4439–4444.
89. Taylor U, Klein S, Petersen S, Kues W, Barcikowski S, Rath D. *Cytometry Part A*. 2010; 77A: 439–446.
90. Porcel E, Liehn S, Remita H, Usami N, Kobayashi K, Furusawa Y, Le Sech C, Lacombe S. *Nanotechnology*. 2010; 21:085103.
91. Park J-E, Atobe M, Fuchigami T. *Electrochimica Acta*. 2005; 51:849–854.
92. Cueto M, Sanz M, Oujja M, Gámez F, Martínez Haya B, Castillejo M. *The Journal of Physical Chemistry C*. 2011; 115:22217–22224.
93. Brown KR, Natan MJ. *Langmuir*. 1998; 14:726–728.
94. Jana NR, Gearheart L, Murphy CJ. *Langmuir*. 2001; 17:6782–6786.
95. Rodriguez-Fernandez J, Perez-Juste J, Garcia de Abajo FJ, Liz-Marzan LM. *Langmuir*. 2006; 22:7007–7010. [PubMed: 16863252]
96. Das AK, Raj CR. *The Journal of Physical Chemistry C*. 2011; 115:21041–21046.
97. Irvani S. *Green Chemistry*. 2011; 13:2638–2650.
98. Kumar KP, Paul W, Sharma CP. *Process Biochemistry*. 2011; 46:2007–2013.
99. Bai H-J, Yang B-S, Chai C-J, Yang G-E, Jia W-L, Yi Z-B. *World Journal of Microbiology and Biotechnology*. 2011; 27:2723–2728.
100. Mokhtari N. *Materials research bulletin*. 2009; 44:1415.
101. Nanda A, Saravanan M. *Nanomedicine: nanotechnology, biology, and medicine*. 2009; 5:452–456.
102. Shahverdi AR, Minaeian S, Shahverdi HR, Jamalifar H, Nohi A-A. *Process Biochemistry*. 2007; 42:919–923.
103. Anil Kumar S, Abyaneh M, Gosavi S, Kulkarni S, Pasricha R, Ahmad A, Khan M. *Biotechnology Letters*. 2007; 29:439–445. [PubMed: 17237973]

104. Mukherjee P, Ahmad A, Mandal D, Senapati S, Sainkar SR, Khan MI, Ramani R, Parischa R, Ajayakumar PV, Alam M, Sastry M, Kumar R. *Angewandte Chemie International Edition*. 2001; 40:3585–3588.
105. Daizy P. *Spectrochimica Acta Part A: Molecular and Biomolecular Spectroscopy*. 2009; 73:374–381.
106. Daizy P. *Spectrochimica Acta Part A: Molecular and Biomolecular Spectroscopy*. 2011; 78:327–331.
107. Bar H, Bhui DK, Sahoo GP, Sarkar P, De SP, Misra A. *Colloids and Surfaces A: Physicochemical and Engineering Aspects*. 2009; 339:134–139.
108. Dubey SP, Lahtinen M, Särkkää H, Sillanpää M. *Colloids and Surfaces B: Biointerfaces*. 2010; 80:26–33.
109. Sharma VK, Yngard RA, Lin Y. *Advances in Colloid and Interface Science*. 2009; 145:83–96. [PubMed: 18945421]
110. Darroudi MA, Abdullah MB, Ibrahim AH, Shameli NAK. *Int J Mol Sci*. 2010; 11:3898–3905. [PubMed: 21152307]
111. Tkachenko AG, Xie H, Coleman D, Glomm W, Ryan J, Anderson MF, Franzen S, Feldheim DL. *Journal of the American Chemical Society*. 2003; 125:4700–4701. [PubMed: 12696875]
112. Bruchez M Jr, Moronne M, Gin P, Weiss S, Alivisatos AP. *Science*. 1998; 281:2013–2016. [PubMed: 9748157]
113. Hong R, Fischer NO, Verma A, Goodman CM, Emrick T, Rotello VM. *Journal of the American Chemical Society*. 2004; 126:739–743. [PubMed: 14733547]
114. De MRS, Akpınar H, Miranda OR, Arvizo RR, Bunz UHF, Rotello VM. *Nat Chem*. 2009; 461–465. [PubMed: 20161380]
115. Ghosh PS, Verma A, Rotello VM. *Chem Commun (Camb)*. 2007; 2796–2798. [PubMed: 17609779]
116. Yang, T.; Mocofanescu, Anca; Shen, Chengmin; Gao, H. *Nanoparticles for Biomedical Applications*. Springer; New York: 2009.
117. Sperling RA, Parak WJ. *Philosophical Transactions of the Royal Society A: Mathematical, Physical and Engineering Sciences*. 2010; 368:1333–1383.
118. Burda C, Chen X, Narayanan R, El-Sayed MA. *ChemInform*. 2005; 36:no–no.
119. Bhattacharyya S, Kudgus R, Bhattacharya R, Mukherjee P. *Pharmaceutical Research*. 2011; 28:237–259. [PubMed: 21104301]
120. Ghosh P, Han G, De M, Kim CK, Rotello VM. *Advanced Drug Delivery Reviews*. 2008; 60:1307–1315. [PubMed: 18555555]
121. Geiser M, Rothen-Rutishauser B, Kapp N, Schurch S, Kreyling W, Schulz H, Semmler M, Hof VI, Heyder J, Gehr P. *Environmental Health Perspectives*. 2005; 113:1555–1560. [PubMed: 16263511]
122. Bartneck M, Keul HA, Singh S, Czaja K, Bornemann J, Bockstaller M, Moeller M, Zwadlo-Klarwasser G, Groll J. *ACS Nano*. 2010; 4:3073–3086. [PubMed: 20507158]
123. Shukla R, Bansal V, Chaudhary M, Basu A, Bhonde RR, Sastry M. *Langmuir*. 2005; 21:10644–10654. [PubMed: 16262332]
124. Carlson C, Hussain SM, Schrand AM, Braydich-Stolle LK, Hess KL, Jones RL, Schlager JJ. *The Journal of Physical Chemistry B*. 2008; 112:13608–13619. [PubMed: 18831567]
125. Yen H-J, Hsu S-h, Tsai C-L. *Small*. 2009; 5:1553–1561. [PubMed: 19326357]
126. Walczyk D, Bombelli FB, Monopoli MP, Lynch I, Dawson KA. *Journal of the American Chemical Society*. 2010; 132:5761–5768. [PubMed: 20356039]
127. Chithrani BD, Ghazani AA, Chan WCW. *Nano Letters*. 2006; 6:662–668. [PubMed: 16608261]
128. Patra HK, Banerjee S, Chaudhuri U, Lahiri P, Dasgupta AK. *Nanomedicine: Nanotechnology, Biology and Medicine*. 2007; 3:111–119.
129. Bhattacharyya S, Singh RD, Pagano R, Robertson JD, Bhattacharya R, Mukherjee P. *Angewandte Chemie International Edition*. 2011:n/a–n/a.
130. Chithrani BD, Chan WCW. *Nano Letters*. 2007; 7:1542–1550. [PubMed: 17465586]

131. Asharani PV, Lianwu Y, Gong Z, Valiyaveettil S. *Nanotoxicology*. 2011; 5:43–54. [PubMed: 21417687]
132. Jiang W, KimBetty YS, Rutka JT, Cha WCW. *Nat Nano*. 2008; 3:145–150.
133. Pelka J, Gehrke H, Esselen M, TuÅárk M, Crone M, BraÃáse S, Muller T, Blank H, Send W, Zibat V, Brenner P, Schneider R, Gerthsen D, Marko D. *Chemical Research in Toxicology*. 2009; 22:649–659. [PubMed: 19290672]
134. Albanase A, Warren CWC. *ACS Nano*. 2011; 5:5478–5489. [PubMed: 21692495]
135. Derjaguin B, Landau L. *Progress in Surface Science*. 1993; 43:30–59.
136. Qiu Y, Liu Y, Wang L, Xu L, Bai R, Ji Y, Wu X, Zhao Y, Li Y, Chen C. *Biomaterials*. 2010; 31:7606–7619. [PubMed: 20656344]
137. Goodman C, McCusker C, Yilmaz T, Rotello V. *Bioconjugate Chem*. 2004; 15:897–900.
138. Verma A, Stellacci F. *Small*. 2010; 6:12–21. [PubMed: 19844908]
139. Verma A, Uzun O, Hu Y, Han H-S, Watson N, Chen S, Irvine DJ, Stellacci F. *Nat Mater*. 2008; 7:588–595. [PubMed: 18500347]
140. Arvizo RR, Miranda OR, Thompson MA, Pabelick CM, Bhattacharya R, Robertson JD, Rotello VM, Prakash YS, Mukherjee P. *Nano Letters*. 2010; 10:2543–2548. [PubMed: 20533851]
141. Monopoli MP, Walczyk D, Campbell A, Elia G, Lynch I, Baldelli Bombelli F, Dawson KA. *J Am Chem Soc*. 2011; 133:2525–2534. [PubMed: 21288025]
142. Kim CK, Ghosh P, Pagliuca C, Zhu Z-J, Menichetti S, Rotello VM. *Journal of the American Chemical Society*. 2009; 131:1360–1361. [PubMed: 19133720]
143. Agasti SS, Chompoosor A, You C-C, Ghosh P, Kim CK, Rotello VM. *Journal of the American Chemical Society*. 2009; 131:5728–5729. [PubMed: 19351115]
144. Arora S, Jain J, Rajwade JM, Paknikar KM. *Toxicology and Applied Pharmacology*. 2009; 236:310–318. [PubMed: 19269301]
145. AshaRani P, Hande MP, Valiyaveettil S. *BMC Cell Biology*. 2009; 10:65. [PubMed: 19761582]
146. Schaller M, Korting HC, Schmid MH. *British Journal of Dermatology*. 1996; 134:445–450. [PubMed: 8731667]
147. Sur I, Cam D, Kahraman M, Baysal A, Culha M. *Nanotechnology*. 2010; 21:175104. [PubMed: 20368680]
148. Lesniak W, Bielinska AU, Sun K, Janczak KW, Shi X, Baker JR, Balogh LP. *Nano Letters*. 2005; 5:2123–2130. [PubMed: 16277438]
149. AshaRani PV, Low Kah Mun G, Hande MP, Valiyaveettil S. *ACS Nano*. 2008; 3:279–290. [PubMed: 19236062]
150. Franco-Molina M, Mendoza-Gamboa E, Sierra-Rivera C, Gomez-Flores R, Zapata-Benavides P, Castillo-Tello P, Alcocer-Gonzalez J, Miranda-Hernandez D, Tamez-Guerra R, Rodriguez-Padilla C. *Journal of Experimental & Clinical Cancer Research*. 2010; 29:148.
151. Greulich C, Diendorf J, Simon T, Eggeler G, Epple M, Köller M. *Acta Biomaterialia*. 2011; 7:347–354. [PubMed: 20709196]
152. De Gusseme B, Sintubin L, Baert L, Thibo E, Hennebel T, Vermeulen G, Uyttendaele M, Verstraete W, Boon N. *Applied and Environmental Microbiology*. 2009; 76:1082–1087. [PubMed: 20038697]
153. Rogers J, Parkinson C, Choi Y, Speshock J, Hussain S. *Nanoscale Research Letters*. 2008; 3:129–133.
154. Bowman M-C, Ballard TE, Ackerson CJ, Feldheim DL, Margolis DM, Melander C. *Journal of the American Chemical Society*. 2008; 130:6896–6897. [PubMed: 18473457]
155. Mallipeddi R, Rohan LC. *Expert Opinion on Drug Delivery*. 2010; 7:37–48. [PubMed: 20017659]
156. Lara H, Ixtepan-Turrent L, Garza-Trevino E, Rodriguez-Padilla C. *Journal of Nanobiotechnology*. 2005; 8:15. [PubMed: 20626911]
157. Elechiguerra J, Burt J, Morones J, Camacho-Bragado A, Gao X, Lara H, Yacaman M. *Journal of Nanobiotechnology*. 2005; 3:6. [PubMed: 15987516]
158. Lara H, Ayala-Nunez N, Ixtepan-Turrent L, Rodriguez-Padilla C. *Journal of Nanobiotechnology*. 2010; 8:1. [PubMed: 20145735]

159. Baram-Pinto D, Shukla S, Perkas N, Gedanken A, Sarid R. *Bioconjugate Chemistry*. 2009; 20:1497–1502. [PubMed: 21141805]
160. Papp I, Sieben C, Ludwig K, Roskamp M, Böttcher C, Schlecht S, Herrmann A, Haag R. *Small*. 2010; 6:2900–2906. [PubMed: 21104827]
161. Sun L, Singh AK, Vig K, Pillai SR, Singh SR. *Journal of Biomedical Nanotechnology*. 2008; 4:149–158.
162. Ferrara N, Kerbel RS. *Nature*. 2005; 438:967–974. [PubMed: 16355214]
163. Ferrara N, Mass RD, Campa C, Kim R. *Annual Review of Medicine*. 2007; 58:491–504.
164. Dvorak HF. *Journal of Clinical Oncology*. 2002; 20:4368–4380. [PubMed: 12409337]
165. Tosetti BRF, Albini A. *Suppl Tumori*. 2002; 1:9–11.
166. Yap CCT, Kay SB. *Nat Rev Cancer*. 2009; 9:167–181. [PubMed: 19238149]
167. Bergers G, Hanahan D. *Nat Rev Cancer*. 2008; 8:592–603. [PubMed: 18650835]
168. Ferrari M. *Nat Rev Cancer*. 2005; 5:161–171. [PubMed: 15738981]
169. Mukherjee P, Bhattacharya R, Wang P, Wang L, Basu S, Nagy JA, Atala A, Mukhopadhyay D, Soker S. *Clinical Cancer Research*. 2005; 11:3530–3534. [PubMed: 15867256]
170. Bhattacharya R, Mukherjee P, Xiong Z, Atala A, Soker S, Mukhopadhyay D. *Nano Letters*. 2004; 4:2479–2481.
171. Arvizo RR, Rana S, Miranda OR, Bhattacharya R, Rotello VM, Mukherjee P. *Nanomedicine: Nanotechnology, Biology and Medicine*. 2010; 7:580–587.
172. Gurunathan S, Lee K-J, Kalishwaralal K, Sheikpranbabu S, Vaidyanathan R, Eom SH. *Biomaterials*. 2009; 30:6341–6350. [PubMed: 19698986]
173. Sriram MI, Kanth SBM, Kalishwaralal K, Gurunathan aS. *Int J Nanomedicine*. 2010; 5:753–762. [PubMed: 21042421]
174. Giuliani N, Storti P, Bolzoni M, Palma B, Bonomini S. *Cancer Microenvironment*. 2011; 4:325–337. [PubMed: 21735169]
175. Jakob C, Sterz J, Zavrski I, Heider U, Kleeberg L, Fleissner C, Kaiser M, Sezer O. *European Journal of Cancer*. 2006; 42:1581–1590. [PubMed: 16797965]
176. Lamorte S, Ferrero2 S, Aschero S, Monitillo L, Bussolati B, Omedé P, Ladetto M, Camussi G. *Leukemia*. 2011:1–10.
177. Bhattacharya R, Patra CR, Verma R, Kumar S, Greipp PR, Mukherjee P. *Advanced Materials*. 2007; 19:711–716.
178. Mukherjee P, Bhattacharya R, Bone N, Lee YK, Patra CR, Wang S, Lu L, Secreto C, Banerjee PC, Yaszemski MJ, Kay NE, Mukhopadhyay D. *J Nanobiotechnology*. 2007; 5:4. [PubMed: 17488514]
179. Sutton B. *Gold Bulletin*. 1986; 19:15–16.
180. Pricker S. *Gold Bulletin*. 1996; 29:53–60.
181. Thakor AS, Jokerst J, Zavaleta C, Massoud TF, Gambhir SS. *Nano Letters*. 2011; 11:4029–4036. [PubMed: 21846107]
182. Tsai C-Y, Shiao A-L, Chen S-Y, Chen Y-H, Cheng P-C, Chang M-Y, Chen D-H, Chou C-H, Wang C-R, Wu C-L. *Arthritis & Rheumatism*. 2007; 56:544–554. [PubMed: 17265489]
183. Jaeger G, Larsen S, Soli N, Moe L. *Acta Veterinaria Scandinavica*. 2007; 49:9. [PubMed: 17381835]
184. Lal S, Clare SE, Halas NJ. *Accounts of Chemical Research*. 2008; 41:1842–1851. [PubMed: 19053240]
185. Manthe RL, Foy SP, Krishnamurthy N, Sharma B, Labhasetwar V. *Molecular Pharmaceutics*. 2010; 7:1880–1898. [PubMed: 20866097]
186. De Rosa F, Bentley MVr. *Pharmaceutical Research*. 2000; 17:1447–1455. [PubMed: 11303952]
187. Huang X, El-Sayed IH, Qian W, El-Sayed MA. *Journal of the American Chemical Society*. 2006; 128:2115–2120. [PubMed: 16464114]
188. Huang X, Jain PK, El-Sayed IH, El-Sayed MA. *Photochemistry and Photobiology*. 2006; 82:412–417. [PubMed: 16613493]



189. Johannsen GUM, Eckelt L, Feussner A, Waldöfner N, Scholz R, Deger WPS, Loening SA, Jordan A. *Int J Hyperthermia*. 2005; 7:637–647. [PubMed: 16304715]
190. Weissleder R. *Nat Biotech*. 2001; 19:316–317.
191. Yatvin MB, Cramp WA. *International Journal of Hyperthermia*. 1993; 9:165–185. [PubMed: 8468503]
192. Fairbairn JJ, Khan MW, Ward KJ, Loveridge BW, Fairbairn DW, O'Neill KL. *Cancer Letters*. 1995; 89:183–188. [PubMed: 7889527]
193. El-Sayed MA. *Accounts of Chemical Research*. 2001; 34:257–264. [PubMed: 11308299]
194. Zinn, S.; Semiattin, S. *Elements of Induction Heating: Design Control and Applications*. ASM International; Ohio: 1988.
195. Chen J, Wang D, Xi J, Au L, Siekkinen A, Warsen A, Li Z-Y, Zhang H, Xia Y, Li X. *Nano Letters*. 2007; 7:1318–1322. [PubMed: 17430005]
196. Pitsillides C, Joe E, Wei X, Anderson R, Lin C. *Biophysical J*. 2003; 84:4023–4032.
197. Raji V, Kumar J, Rejiya CS, Vibin M, Shenoj VN, Abraham A. *Experimental Cell Research*. 2011; 317:2052–2058. [PubMed: 21565190]
198. Bartczak D, Muskens OL, Nitti S, Sanchez-Elsner T, Millar TM, Kanaras AG. *Small*. 2011; 10:1002/sml.201101422
199. von Maltzahn G, Park J-H, Agrawal A, Bandaru NK, Das SK, Sailor MJ, Bhatia SN. *Cancer Research*. 2009; 69:3892–3900. [PubMed: 19366797]
200. Sirotkina MA, Elagin VV, Shirmanova MV, Bugrova ML, Snopova LB, Kamensky VA, Nadtochenko VA, Denisov NN, Zagaynova EV. *Journal of Biophotonics*. 2010; 3:718–727. [PubMed: 20626005]
201. Bernardi P, Cavagnaro M, Pisa S, Piuze E. *Biomedical Engineering, IEEE Transactions on*. 2003; 50:295–304.
202. Cardinal J, Klune JR, Chory E, Jeyabalan G, Kanzius JS, Nalesnik M, Geller DA. *Surgery*. 2008; 144:125–132. [PubMed: 18656617]
203. Murphy CJ, Gole AM, Stone JW, Sisco PN, Alkilany AM, Goldsmith EC, Baxter SC. *Accounts of Chemical Research*. 2008; 41:1721–1730. [PubMed: 18712884]
204. Maltzahn, Gv; Centrone, A.; Park, J-H.; Ramanathan, R.; Sailor, MJ.; Hatton, TA.; Bhatia, SN. *Advanced Materials*. 2009; 21:3175–3180. [PubMed: 20174478]
205. Cho HS. *Physics in Medicine and Biology*. 2005; 50:N163. [PubMed: 16030374]
206. Hainfeld JF, Slatkin DN, Focella TM, Smilowitz HM. *Br J Radiol*. 2006; 79:248–253. [PubMed: 16498039]
207. Kong T, Zeng J, Wang X, Yang X, Yang J, McQuarrie S, McEwan A, Roa W, Chen J, Xing JZ. *Small*. 2008; 4:1537–1543. [PubMed: 18712753]
208. Matlachov AN, Volegov PL, Espy MA, George JS, Kraus RH Jr. *Journal of Magnetic Resonance*. 2004; 170:1–7. [PubMed: 15324752]
209. Katti K, Kannan R, Katti K, Kattumori V, Pandrapraganda R, Rahing V, Cutler C, Boote E, Casteel S, Smith C, Robertson J, Jurrison S. *Czechoslovak Journal of Physics*. 2006; 56:D23–D34.
210. Gannon C, Patra C, Bhattacharya R, Mukherjee P, Curley S. *Journal of Nanobiotechnology*. 2008; 6:1–9. [PubMed: 18173857]
211. Chi-Jen L, Chang-Hai W, Chia-Chi C, Tsung-Yeh Y, Shin-Tai C, Wei-Hua L, Cheng-Feng L, Kuen-Ho L, Hwu Y, Yao-Chang L, Chia-Liang C, Chung-Shi Y, Chen YJ, Je JH, Margaritondo G. *Nanotechnology*. 2008; 19:295104. [PubMed: 21730596]
212. Chi-Jen L, Chang-Hai W, Shin-Tai C, Hsiang-Hsin C, Wei-Hua L, Chia-Chi C, Cheng-Liang W, Ivan MK, Hwu Y, Tsung-Ching L, Michael H, Chung-Shi Y, Yu-Jen C, Margaritondo G. *Physics in Medicine and Biology*. 2010; 55:931. [PubMed: 20090183]
213. Polf JC, Bronk LF, Driessen WHP, Arap W, Pasqualini R, Gillin M. *Applied Physics Letters*. 2011; 98:193702–193703. [PubMed: 21915155]
214. Xu R, Ma J, Sun X, Chen Z, Jiang X, Guo Z, Huang L, Li Y, Wang M, Wang C, Liu J, Fan X, Gu J, Chen X, Zhang Y, Gu N. *Cell Res*. 2009; 19:1031–1034. [PubMed: 19621033]

215. Liu L, Ni F, Zhang J, Jiang X, Lu X, Guo Z, Xu R. *Acta Biochimica et Biophysica Sinica*. 2011; 43:316–323. [PubMed: 21377996]
216. Chithrani DB, Jelveh S, Jalali F, van Prooijen M, Allen C, Bristow RG, Hill RP, Jaffray DA. *Radiation Research*. 2010; 173:719–728. [PubMed: 20518651]
217. Porcel E, Kobayashi K, Usami N, Remita H, Sech CL, Lacombe S. *Journal of Physics: Conference Series*. 261:012004.
218. Asharani PV, Xinyi N, Hande MP, Valiyaveetil S. *Nanomedicine*. 2010; 5:51–64. [PubMed: 20025464]
219. Hainfeld JF, Slatkin DN, Smilowitz HM. *Physics in Medicine and Biology*. 2004; 49:N309. [PubMed: 15509078]
220. Paciotti GF, Myer L, Weinreich D, Goia D, Pavel N, McLaughlin RE, Tamarkin L. *Drug Delivery*. 2004; 11:169–183. [PubMed: 15204636]
221. Zhang G, Yang Z, Lu W, Zhang R, Huang Q, Tian M, Li L, Liang D, Li C. *Biomaterials*. 2009; 30:1928–1936. [PubMed: 19131103]
222. Villiers C, Freitas H, Couderc R, Villiers MB, Marche P. *J Nanopart Res*. 2010; 12:55–60. [PubMed: 21841911]
223. Pan Y, Leifert A, Ruau D, Neuss S, Bornemann J, Schmid G, Brandau W, Simon U, Jahnen-Dechent W. *Small*. 2009; 5:2067–2076. [PubMed: 19642089]
224. Ng C-T, Dheen ST, Yip W-CG, Ong C-N, Bay B-H, Lanry Yung L-Y. *Biomaterials*. 2011; 32:7609–7615. [PubMed: 21764123]
225. Li JJ, Hartono D, Ong C-N, Bay B-H, Yung L-YL. *Biomaterials*. 2010; 31:5996–6003. [PubMed: 20466420]
226. Zhang Q, Hitchins VM, Schrand AM, Hussain SM, Goering PL. *Nanotoxicology*. 2011; 5:284–295. [PubMed: 20849214]
227. Schaeublin NM, Braydich-Stolle LK, Schrand AM, Miller JM, Hutchison J, Schlager JJ, Hussain SM. *Nanoscale*. 2011; 3:410–420. [PubMed: 21229159]
228. Chomposor A, Saha K, Ghosh PS, Macarthy DJ, Miranda OR, Zhu Z-J, Arcaro KF, Rotello VM. *Small*. 2010; 6:2246–2249. [PubMed: 20818619]
229. Hussain SM, Hess KL, Gearhart JM, Geiss KT, Schlager JJ. *Toxicology in Vitro*. 2005; 19:975–983. [PubMed: 16125895]
230. Park E-J, Yi J, Kim Y, Choi K, Park K. *Toxicology in Vitro*. 2010; 24:872–878. [PubMed: 19969064]
231. Piao MJ, Kang KA, Lee IK, Kim HS, Kim S, Choi JY, Choi J, Hyun JW. *Toxicol Lett*. 2011; 201:92–100. [PubMed: 21182908]
232. Teodoro, JoS; Simões, AM.; Duarte, FV.; Rolo, AP.; Murdoch, RC.; Hussain, SM.; Palmeira, CM. *Toxicology in Vitro*. 2011; 25:664–670. [PubMed: 21232593]
233. Zhang R, Piao MJ, Kim KC, Kim AD, Choi J-Y, Choi J, Hyun JW. *The International Journal of Biochemistry & Cell Biology*. 2012; 44:224–232.
234. Rosas-Hernandez H, Jimenez-Badillo S, Martinez-Cuevas PP, Gracia-Espino E, Terrones H, Terrones M, Hussain SM, Ali SF, Gonzalez C. *Toxicol Lett*. 2009; 191:305–313. [PubMed: 19800954]
235. Berry CC, Charles S, Wells S, Dalby MJ, Curtis ASG. *International Journal of Pharmaceutics*. 2004; 269:211–225. [PubMed: 14698593]
236. Braydich-Stolle LK, Lucas B, Schrand A, Murdock RC, Lee T, Schlager JJ, Hussain SM, Hofmann M-C. *Toxicological Sciences*. 116:577–589.
237. Speshock J, Braydich-Stolle L, Szymanski E, Hussain S. *Nanoscale Research Letters*. 2011; 6:1–7.
238. Comfort KK, Maurer EI, Braydich-Stolle LK, Hussain SM. *ACS Nano*. 2011
239. Gottlieb NL. *Scand J Rheumatol Suppl*. 1983; 51:10–14. [PubMed: 6426043]
240. Champion GD, Graham GG, Ziegler JB. *Baillieres Clin Rheumatol*. 1990; 4:491–534. [PubMed: 2093439]
241. Kean WF, Kean IR. *Inflammopharmacology*. 2008; 16:112–125. [PubMed: 18523733]

242. Walz DT, DiMartino MJ, Griswold DE, Intoccia AP, Flanagan TL. *Am J Med.* 1983; 75:90–108. [PubMed: 6318557]
243. Palmer DG, Dunckley JV. *Aust N Z J Med.* 1973; 3:461–466. [PubMed: 4204711]
244. Blocka K, Furst DE, Landaw E, Dromgoole S, Blomberg A, Paulus HE. *J Rheumatol Suppl.* 1982; 8:110–119. [PubMed: 6813473]
245. Gottlieb NL. *J Rheumatol Suppl.* 1982; 8:99–109. [PubMed: 6813498]
246. Penneys NS, Kramer K, Gottlieb NL. *J Invest Dermatol.* 1975; 65:331–333. [PubMed: 808577]
247. Gottlieb NL, Smith PM, Smith EM. *Arthritis Rheum.* 1972; 15:582–592. [PubMed: 4628731]
248. Semmler-Behnke M, Kreyling WG, Lipka J, Fertsch S, Wenk A, Takenaka S, Schmid G, Brandau W. *Small.* 2008; 4:2108–2111. [PubMed: 19031432]
249. Zhang XD, Wu HY, Wu D, Wang YY, Chang JH, Zhai ZB, Meng AM, Liu PX, Zhang LA, Fan FY. *International Journal of Nanomedicine.* 2010; 5:771–781. [PubMed: 21042423]
250. Loeschner K, Hadrup N, Qvortrup K, Larsen A, Gao X, Vogel U, Mortensen A, Lam HR, Larsen EH. *Particle and Fibre Toxicology.* 2011; 8:18. [PubMed: 21631937]
251. Chrastina A, Schnitzer JE. *International Journal of Nanomedicine.* 2010; 5:653–659. [PubMed: 20856841]
252. Sung JH, Ji JH, Yoon JU, Kim DS, Song MY, Jeong J, Han BS, Han JH, Chung YH, Kim J, Kim TS, Chang HK, Lee EJ, Lee JH, Yu IJ. *Inhalation Toxicology.* 2008; 20:567–574. [PubMed: 18444009]
253. Sung JH, Ji JH, Park JD, Yoon JU, Kim DS, Jeon KS, Song MY, Jeong J, Han BS, Han JH, Chung YH, Chang HK, Lee JH, Cho MH, Kelman BJ, Yu IJ. *Toxicological Sciences.* 2009; 108:452–461. [PubMed: 19033393]
254. Sung, Jae Hyuck; Ji, Jun Ho; Song, Kyung Seuk; Lee, Ji Hyun; Choi, Kyung Hee; Lee, Sang Hee; Yu, Il Je. *Toxicology and Industrial Health.* 2011; 27:149–154. [PubMed: 20870693]
255. Kim YS, Kim JS, Cho HS, Rha DS, Kim JM, Park JD, Choi BS, Lim R, Chang HK, Chung YH, Kwon IH, Jeong J, Han BS, Yu IJ. *Inhalation toxicology.* 2008; 20:575–583. [PubMed: 18444010]
256. Kim YS, Song MY, Park JD, Song KS, Ryu HR, Chung YH, Chang HK, Lee JH, Oh KH, Kelman BJ, Hwang IK, Yu IJ. *Particle and Fibre Toxicology.* 2010; 7:20. [PubMed: 20691052]
257. De Jong WH, Hagens WI, Krystek P, Burger MC, An JA, Sips M, Geertsma RE. *Biomaterials.* 2008; 29:1912–1919. [PubMed: 18242692]
258. Pan Y, Neuss S, Leifert A, Fischler M, Wen F, Simon U, Schmid G, Brandau W, Jahnen-Dechent W. *Small.* 2007; 3:1941–1949. [PubMed: 17963284]
259. Abdelhalim MA, Jarrar B. *Lipids in Health and Disease.* 2011; 10:147. [PubMed: 21859444]
260. Chen YS, Hung YC, Liau I, Huang GS. *Nanoscale research letters.* 2009; 4:858–864. [PubMed: 20596373]
261. Perrault SD, Walkey C, Jennings T, Fischer HC, Chan WCW. *Nano Letters.* 2009; 9:1909–1915. [PubMed: 19344179]
262. Park EJ, Bae E, Yi J, Kim Y, Choi K, Lee SH, Yoon J, Lee BC, Park K. *Environ Toxicol Pharmacol.* 2010; 30:162–168. [PubMed: 21787647]
263. Lankveld DP, Oomen AG, Krystek P, Neigh A, Troost-de Jong A, Noorlander CW, Van Eijkeren JC, Geertsma RE, De Jong WH. *Biomaterials.* 2010; 31:8350–8361. [PubMed: 20684985]
264. Gosens I, Post JA, de la Fonteyne L, Jansen E, Geus J, Cassee F, de Jong W. *Particle and Fibre Toxicology.* 2010; 7:37. [PubMed: 21126342]
265. Balogh L, Nigavekar SS, Nair BM, Lesniak W, Zhang C, Sung LY, Kariapper MST, El-Jawahri A, Llanes M, Bolton B, Mamou F, Tan W, Hutson A, Minc L, Khan MK. *Nanomedicine: Nanotechnology, Biology and Medicine.* 2007; 3:281–296.
266. Arvizo RR, Miranda OR, Moyano DF, Walden CA, Giri K, Bhattacharya R, Robertson JD, Rotello VM, Reid JM, Mukherjee P. *PLoS ONE.* 2011; 6:e24374. [PubMed: 21931696]
267. Hirn S, Semmler-Behnke M, Schleh C, Wenk A, Lipka J, Schäffler M, Takenaka S, Möller W, Schmid Gn, Simon U, Kreyling WG. *European Journal of Pharmaceutics and Biopharmaceutics.* 2011; 77:407–416. [PubMed: 21195759]

268. Zhu Z-J, Carboni R, Quercio MJ, Yan B, Miranda OR, Anderton DL, Arcaro KF, Rotello VM, Vachet RW. *Small*. 2010; 6:2261–2265. [PubMed: 20842664]
269. Sharma, HS.; Hussain, S.; Schlager, J.; Ali, SF.; Sharma, A.; Czernicki, Z.; Baethmann, A.; Ito, U.; Katayama, Y.; Kuroiwa, T.; Mendelow, D. *Brain Edema XIV*. Steiger, HJ., editor. Vol. 106. Springer; Vienna: 2010. p. 359-364.
270. Sharma HS, Ali SF, Hussain SM, Schlager JJ, Sharma A. *Journal of Nanoscience and Nanotechnology*. 2009; 9:5055–5072. [PubMed: 19928185]
271. Tang XLJ, Wang S, Wang J, Liu L, Li J, Yuan F, Xi T. *J Nanosci Nanotechnology*. 2009; 9:4924–4932.
272. Garza-Ocanas L, Ferrer DA, Burt J, Diaz-Torres LA, Ramirez Cabrera M, Rodriguez VT, Lujan Rangel R, Romanovicz D, Jose-Yacamán M. *Metallomics*. 2009; 2:204–210. [PubMed: 21069158]
273. Lasagna-Reeves C, Gonzalez-Romero D, Barria MA, Olmedo I, Clos A, Sadagopa Ramanujam VM, Urayama A, Vergara L, Kogan MJ, Soto C. *Biochemical and Biophysical Research Communications*. 2010; 393:649–655. [PubMed: 20153731]
274. Trickler WJ, Lantz SM, Murdock RC, Schrand AM, Robinson BL, Newport GD, Schlager JJ, Oldenburg SJ, Paule MG, Slikker W, Hussain SM, Ali SF. *Toxicological Sciences*. 2010; 118:160–170. [PubMed: 20713472]
275. Korani M, Rezayat SM, Gilani K, Arbabi Bidgoli S, Adeli S. *International Journal of Nanomedicine*. 2011; 6:855–862. [PubMed: 21720498]
276. Samberg ME, Oldenburg SJ, Monteiro-Riviere NA. *Environ Health Perspect*. 2009; 118.
277. Larese FF, D'Agostin F, Crosera M, Adami G, Renzi N, Bovenzi M, Maina G. *Toxicology*. 2009; 255:33–37. [PubMed: 18973786]
278. Sonavane G, Tomoda K, Sano A, Ohshima H, Terada H, Makino K. *Colloids and Surfaces B: Biointerfaces*. 2008; 65:1–10.
279. Sonavane G, Tomoda K, Makino K. *Colloids and Surfaces B: Biointerfaces*. 2008; 66:274–280.
280. Ahamed M, Alsalthi MS, Siddiqui MK. *Clin Chim Acta*. 2010; 411:1841–1848. [PubMed: 20719239]
281. Gorth DJ, Rand DM, Webster TJ. *International Journal of Nanomedicine*. 2011; 6:343–350. [PubMed: 21383859]
282. Lee KJ, Nallathamby PD, Browning LM, Osgood CJ, Xu XH. *ACS Nano*. 2007; 1:133–143. [PubMed: 19122772]
283. Asharani PV, Lian Wu Y, Gong Z, Valiyaveetil S. *Nanotechnology*. 2008; 19:255102. [PubMed: 21828644]
284. Sung JH, Ji JH, Yoon JU, Kim DS, Song MY, Jeong J, Han BS, Han JH, Chung YH, Kim J, Kim TS, Chang HK, Lee EJ, Lee JH, Yu IJ. *Inhalation toxicology*. 2008; 20:567–574. [PubMed: 18444009]
285. Wu Y, Zhou Q, Li H, Liu W, Wang T, Jiang G. *Aquat Toxicol*. 2010; 100:160–167. [PubMed: 20034681]
286. Scown TM, Santos EM, Johnston BD, Gaiser B, Baalousha M, Mitov S, Lead JR, Stone V, Fernandes TF, Jepson M, van Aerle R, Tyler CR. *Toxicological Sciences*. 2010; 115:521–534. [PubMed: 20219766]
287. Ringwood AH, McCarthy M, Bates TC, Carroll DL. *Marine Environmental Research*. 2010; 69(Supplement 1):S49–S51. [PubMed: 19913905]
288. Roh JY, Sim SJ, Yi J, Park K, Chung KH, Ryu DY, Choi J. *Environ Sci Technol*. 2009; 43:3933–3940. [PubMed: 19544910]
289. Browning LM, Lee KJ, Huang T, Nallathamby PD, Lowman JE, Nancy Xu X-H. *Nanoscale*. 2009; 1:138–152. [PubMed: 20644873]
290. BLUMBERG H, CAREY TN. *Journal of the American Medical Association*. 1934; 103:1521–1524.
291. Rosenman KD, Moss A, Kon S. *J Occup Med*. 1979; 21:430–435. [PubMed: 469606]
292. Rosenman KD, Seixas N, Jacobs I. *Br J Ind Med*. 1987; 44:267–272. [PubMed: 3567102]

293. Moss AP, Sugar A, Hargett NA, Atkin A, Wolkstein M, Rosenman KD. *Arch Ophthalmol.* 1979; 97:906–908. [PubMed: 312638]
294. Chang AL, Khosravi V, Egbert B. *J Cutan Pathol.* 2006; 33:809–811. [PubMed: 17177941]
295. Tang J, Xi T. *Journal of biomedical engineering.* 2008; 25:958–961. [PubMed: 18788318]
296. Lee H-Y, Choi Y-J, Jung E-J, Yin H-Q, Kwon J-T, Kim J-E, Im H-T, Cho M-H, Kim J-H, Kim H-Y, Lee B-H. *Journal of Nanoparticle Research.* 2010; 12:1567–1578.
297. Rahman MF, Wang J, Patterson TA, Saini UT, Robinson BL, Newport GD, Murdock RC, Schlager JJ, Hussain SM, Ali SF. *Toxicol Lett.* 2009; 187:15–21. [PubMed: 19429238]
298. Rosi NL, Giljohann DA, Thaxton CS, Lytton-Jean AK, Han MS, Mirkin CA. *Science.* 2006; 312:1027–1030. [PubMed: 16709779]
299. Rapson WS. *Contact Dermatitis.* 1985; 13:56–65. [PubMed: 3905247]
300. Merchant B. *Biologicals.* 1998; 26:49–59. [PubMed: 9637749]
301. Heuer MA, Pietrusko RG, Morris RW, Scheffler BJ. *J Rheumatol.* 1985; 12:695–699. [PubMed: 3932651]
302. Antonovych TT. *Ann Clin Lab Sci.* 1981; 11:386–391. [PubMed: 7036839]
303. Horton RJ. *Scand J Rheumatol Suppl.* 1983; 51:100–110. [PubMed: 6426044]
304. Szabo KT, Guerriero FJ, Kang YJ. *Vet Pathol Suppl.* 1978; 15:89–96. [PubMed: 108854]
305. Lanone S, Boczkowski J. *Curr Mol Med.* 2006; 6:651–663. [PubMed: 17022735]
306. Dobrovolskaia MA, McNeil SE. *Nat Nanotechnol.* 2007; 2:469–478. [PubMed: 18654343]
307. Gottlieb NL, Smith PM, Penneys NS, Smith EM. *Arthritis Rheum.* 1974; 17:56–62. [PubMed: 4272627]
308. Gottlieb NL, Smith PM, Smith EM. *Arthritis Rheum.* 1972; 15:16–22. [PubMed: 5059639]
309. Mascarenhas BR, Granda JL, Freyberg RH. *Arthritis Rheum.* 1972; 15:391–402. [PubMed: 5046469]
310. Graham GG, Champion GD, Haavisto TM, McNaught PJ. *Ann Rheum Dis.* 1981; 40:210. [PubMed: 7224692]
311. Li Y-F, Chen C. *Small.* 2011; 7:2965–2980. [PubMed: 21932238]
312. Hussain SM, Javorina AK, Schrand AM, Duhart HM, Ali SF, Schlager JJ. *Toxicol Sci.* 2006; 92:456–463. [PubMed: 16714391]
313. Jayakumar AR, Rama Rao KV, Kalaiselvi P, Norenberg MD. *Neurochem Res.* 2004; 29:2051–2056. [PubMed: 15662839]
314. Wang J, Rahman MF, Duhart HM, Newport GD, Patterson TA, Murdock RC, Hussain SM, Schlager JJ, Ali SF. *Neurotoxicology.* 2009; 30:926–933. [PubMed: 19781568]
315. Prabhu BM, Ali SF, Murdock RC, Hussain SM, Srivatsan M. *Nanotoxicology.* 2010; 4:150–160. [PubMed: 20543894]
316. Chen Z, Meng H, Xing G, Chen C, Zhao Y, Jia G, Wang T, Yuan H, Ye C, Zhao F, Chai Z, Zhu C, Fang X, Ma B, Wan L. *Toxicol Lett.* 2006; 163:109–120. [PubMed: 16289865]
317. Meng H, Chen Z, Xing G, Yuan H, Chen C, Zhao F, Zhang C, Zhao Y. *Toxicol Lett.* 2007; 175:102–110. [PubMed: 18024012]
318. Summers HD, Rees P, Holton MD, Brown RM, Chappell SC, Smith PJ, Errington RJ. *Nature Nanotechnol.* 2011; 6:170–174. [PubMed: 21258333]

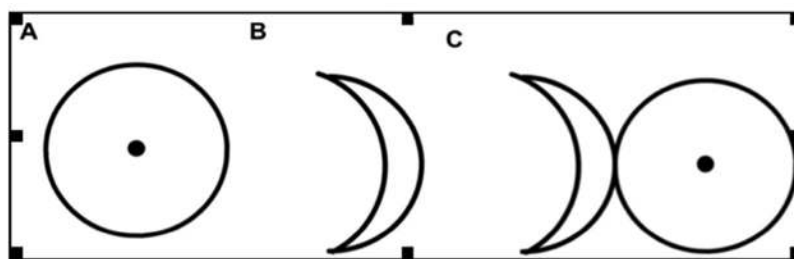


**Fig 1.**  
Alchemy symbol of (A) Gold, (B) Silver, (C) Platinum.

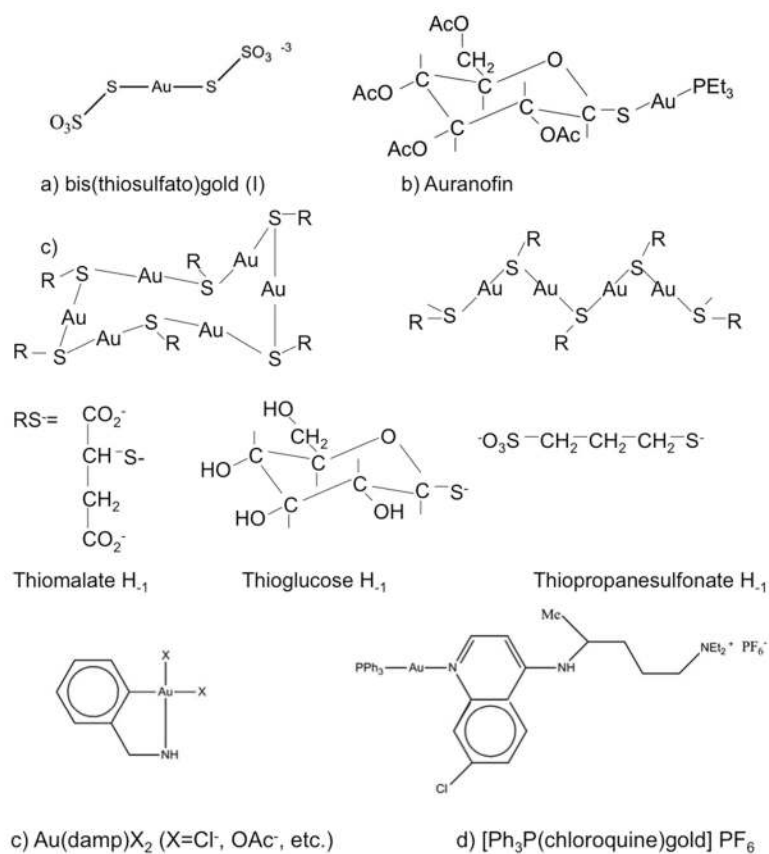


**Fig 2.** Structures of Gold complexes with antiarthritic, antitumor, and antimalarial activity. (a, b) antiarthritic drugs; (c) gold (III) antitumor agents; (d) antimalarial complex of chloroquine.



**Fig 3.** The Lycurgus Cup 1958,1202.1 in reflected (a) and transmitted (b) light. Scene showing Lycurgus being enmeshed by Ambrosia, now transformed into a vine-shoot. Department of Prehistory and Europe, The British Museum. Height: 16.5 cm (with modern metal mounts), diameter: 13.2 cm. Reprinted with permission from © Trustees of the British Museum



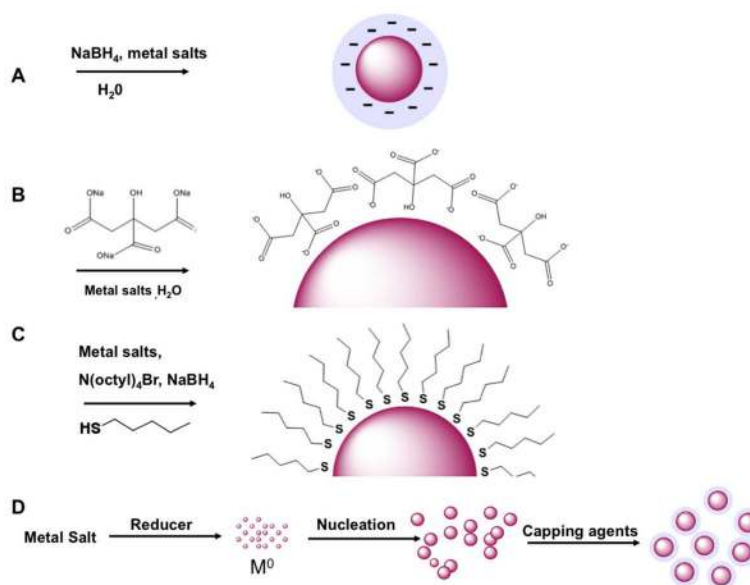


**Fig 4.** Representative chemical reduction schematics for nanoparticle synthesis. (A) Basic reduction of metal salts. (B) Reduction using sodium citrate that is also the capping agent. (C) Reduction and synthesis using non-polar ligands: in this example, a nonpolar thiol. (D) Chemical ripening using particle seeding and nucleation.

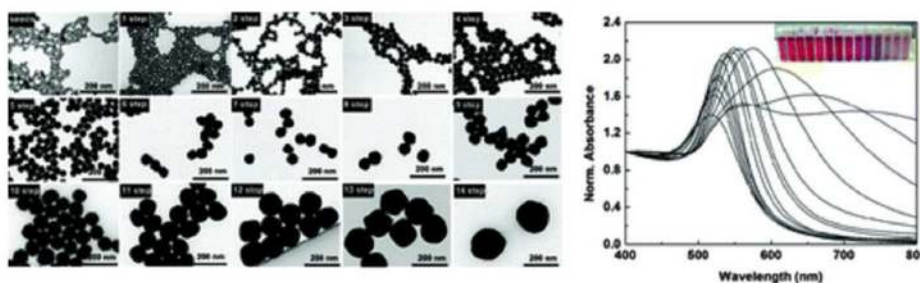


**Fig 5.**

Monodisperse citrate-stabilized gold nanoparticles with a uniform quasi-spherical shape of up to 200 nm and a narrow size distribution were synthesized following a kinetically controlled seeded growth strategy via the reduction of  $\text{HAuCl}_4$  by sodium citrate. The inhibition of any secondary nucleation during homogeneous growth was controlled by adjusting the reaction conditions: temperature, gold precursor to seed particle concentration, and pH. This method presents improved results regarding the traditional Frens method in several aspects: (i) it produces particles of higher monodispersity; (ii) it allows better control of the gold nanoparticle size and size distribution; and (iii) it leads to higher concentrations. Gold nanoparticles synthesized following this method can be further functionalized with a wide variety of molecules, hence this method appears to be a promising candidate for application in the fields of biomedicine, photonics, and electronics, among others. Reprinted with permission from ref. 37. Copyright © 2011 American Chemical Society.

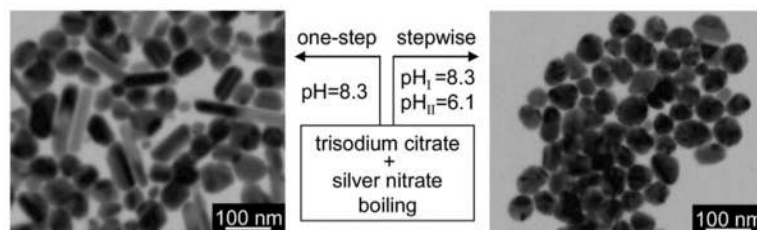


**Fig. 6.**

Growth of silver nanoparticles by the citrate reduction of silver nitrate under the range of pH from 5.7 to 11.1 was investigated systematically and quantitatively. Reduction of the silver precursor ( $\text{Ag}^+$ ) was promoted with increased pH, attributed to the higher activity of the citrate reductant under high pH value. Under high pH, the product was composed of both spherical and rod-like silver nanoparticles as a result of the fast reduction rate of the precursor. Under low pH, the product was mainly dominated by triangle or polygon silver nanoparticles due to the slow reduction rate of the precursor. The product that is dominated by spherical silver nanoparticles cannot be acquired by the one-step citrate reduction method in the range of pH investigated, indicating the poor balance between the nucleation and growth processes in the reactions. On the basis of the results of quantitative analyses, a stepwise reduction method, in which the nucleation and growth processes were carried out at high and low pH, respectively, was proposed for the syntheses of spherical silver nanoparticles. Reprinted with permission from ref. 65. Copyright © 2009 American Chemical Society.

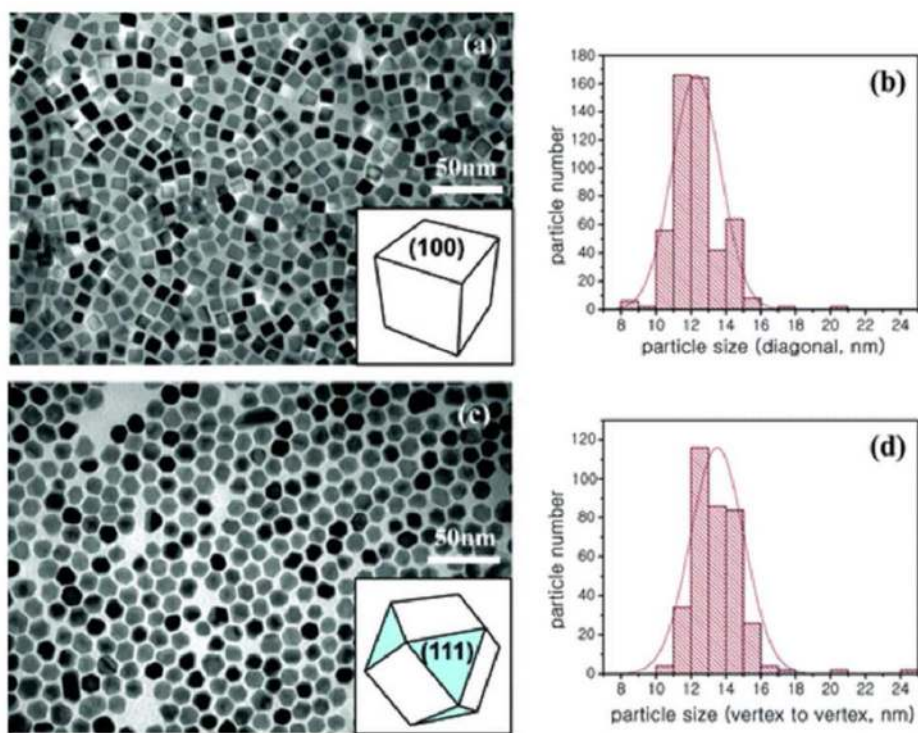


**Fig. 7.** (a) TEM image and (b) size distribution of TTAB-stabilized cubic particles (average size:  $12.3 \pm 1.4$  nm, 79% cubes, 3% triangles, and 18% irregular shapes). (c) TEM image and (d) size distribution of TTAB-stabilized cuboctahedral particles (average size:  $13.5 \pm 1.5$  nm, 90% cuboctahedra and 10% irregular shapes). Reprinted with permission from ref. 77. Copyright © 2007 American Chemical Society.

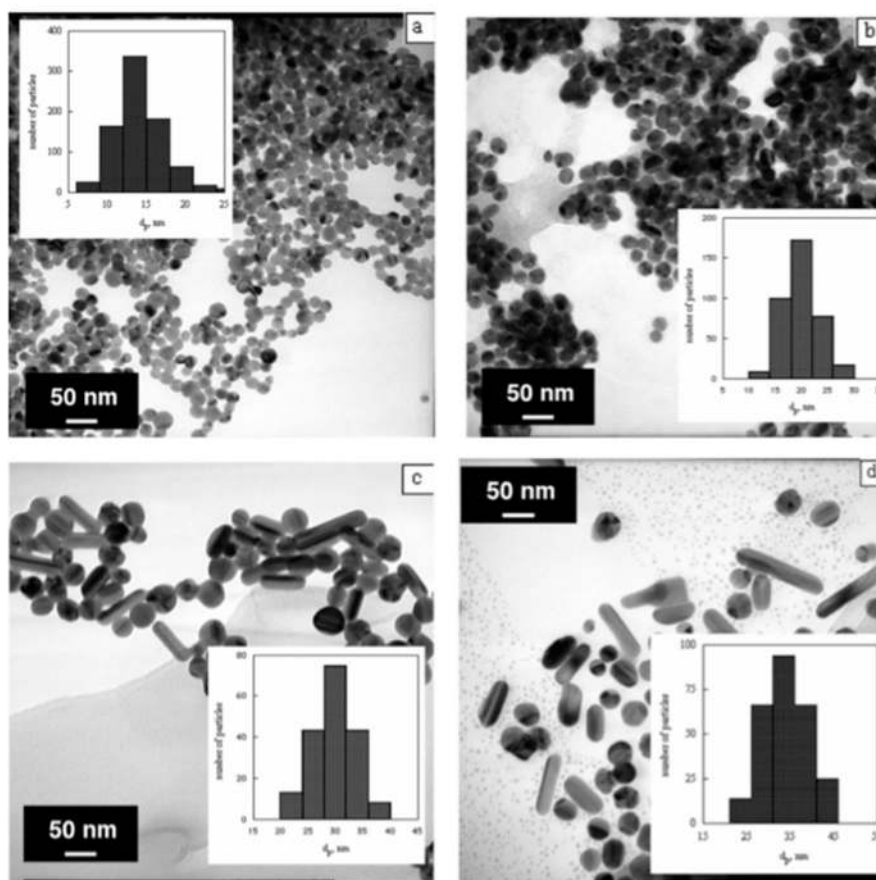


**Fig. 8.** TEM photographs for four colloids prepared in one-step syntheses with different  $n^+/n_s$  ratios: (a)  $n^+/n_s = 3.6$ ; (b)  $n^+/n_s = 18.9$ ; (c)  $n^+/n_s = 32.4$ ; (d)  $n^+/n_s = 45$ . All photographs have the same magnification. The inserts are the histograms of particle size distribution calculated only for spherical particles. Reprinted with permission from ref. 83. Copyright © 2007 American Chemical Society.

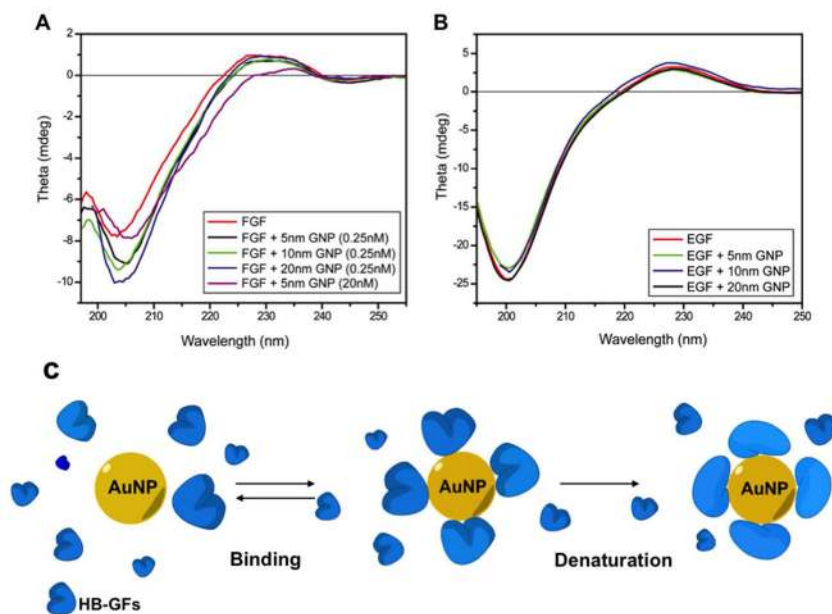


**Fig. 9.** Binding of heparin-binding growth factors (HB-GFs) to gold nanoparticles leads to the inhibition of their function due to change in the protein structure (A,B) Far UV-CD spectra was measured from 180 to 250 nm in a 1 cm cuvette. (A) 0.2 mg/mL bFGF were incubated with and without GNPs in 5 mM phosphate buffer. (B) 0.15 mg/mL EGF were incubated with and without GNPs under similar conditions as listed above. The blanks containing GNPs with same concentration in buffer were subtracted from each data set. (C) Cartoon representation of protein denaturation on the surface of AuNPs. Modified with permission from ref. 171. Copyright © 2011 Elsevier.

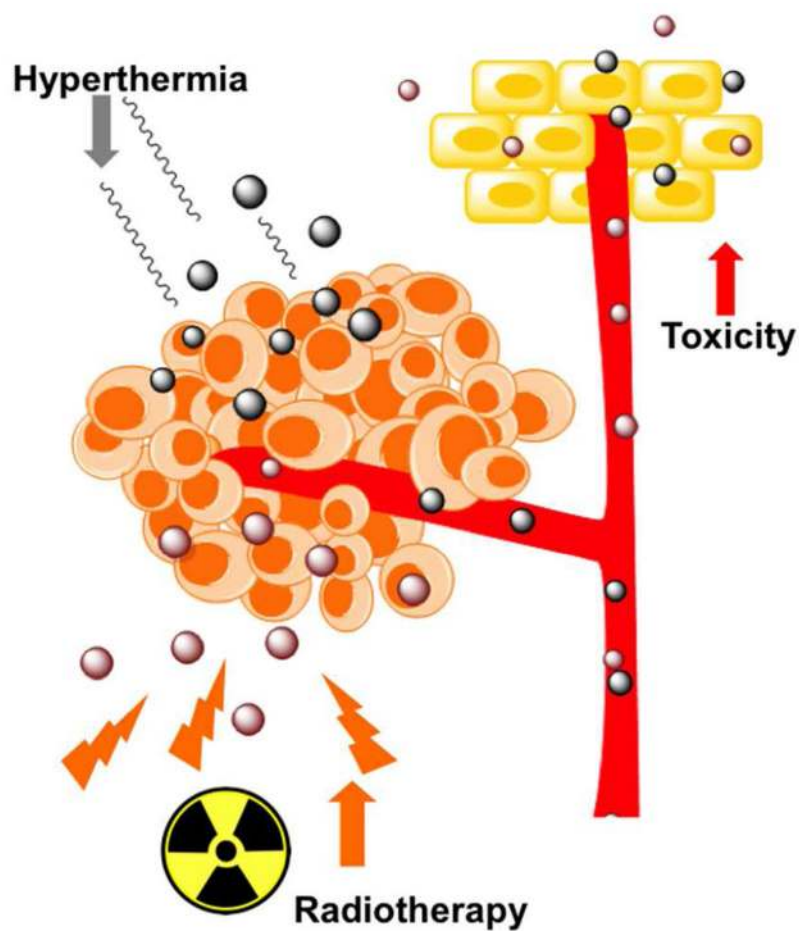


**Fig. 10.** Use of noble metal nanoparticles for therapy. Tumors can be targeted with nanoparticles to induce hyperthermia and enhance radiotherapy. However, non-specific targeting of the nanoparticles may have severe toxic effects on healthy cells.

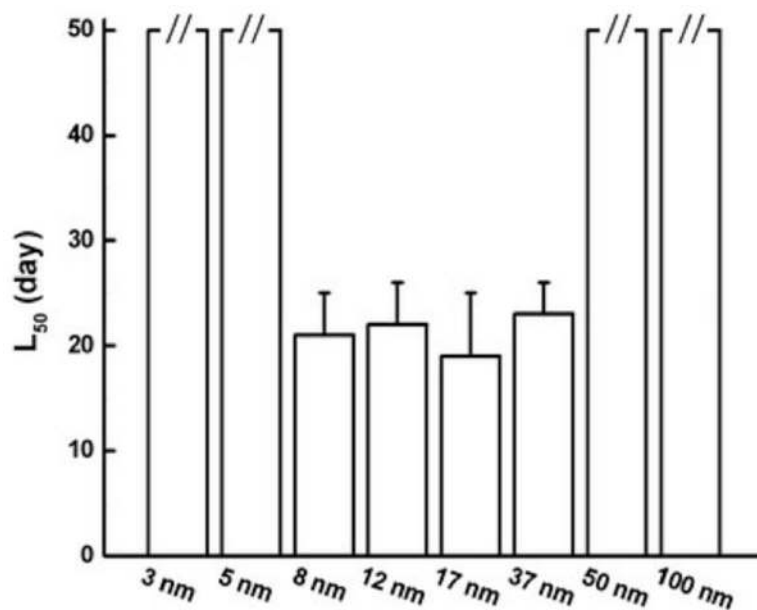


**Fig. 11.**

Average lifespan of mice receiving AuNPs with diameters between 8 and 37 nm was shortened to different extents. The average lifespan ( $L_{50}$ ) was defined as the time beyond which half of the mice died. Mice injected with GNPs outside the lethal range behaved normally. The break marks on the top of bars indicate no death observed during the experimental period. Reprinted with permission from ref. 260. Copyright © 2009 Springer.



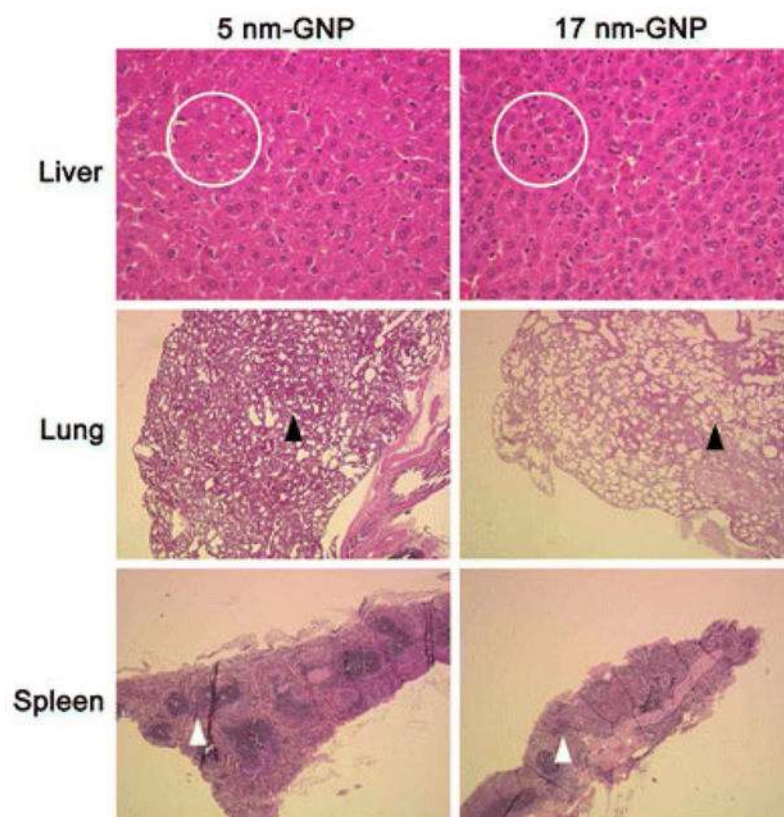


**Fig. 12.** H&E staining showed AuNP-induced abnormality in major organs. (Top to bottom) HE staining for liver, lung, and spleen. The left column shows tissues from 5 nm GNP-treated animals. The right column shows tissues from 17 nm GNP-treated mice. Reprinted with permission from ref. 260. Copyright © 2009 Springer.

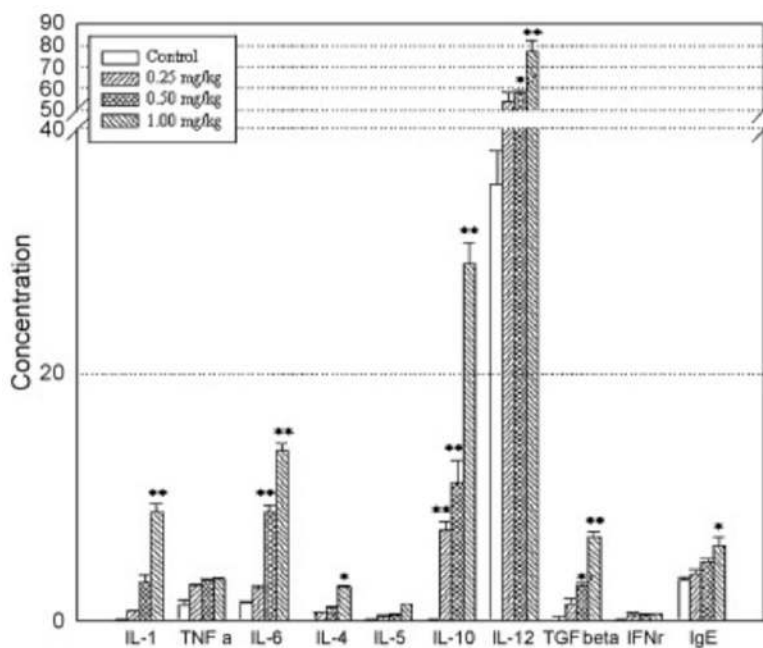


**Fig. 13.**

The serum levels of cytokines and IgE after oral administration of AgNPs (42 nm). Mice were treated with AgNPs with different doses of 0.25 mg/kg, 0.5 mg/kg, and 1 mg/kg for 28 days. Mice were sacrificed after treatment of 28 days and experiments were performed using 3 samples. The concentration unit of cytokines is pg/ml and that of IgE is ng/ml serum. Significantly different from control group, \* $P < 0.05$ , \*\* $P < 0.01$ . Reprinted with permission from ref. 262. Copyright 2010 Elsevier.

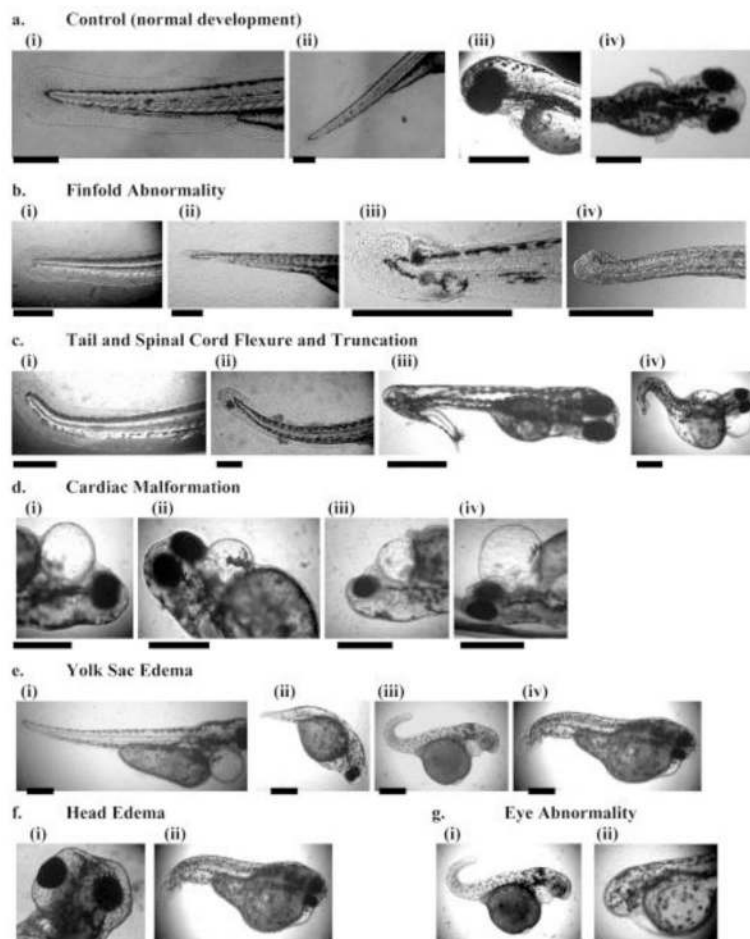


**Fig. 14.** Representative optical images of (a) normally developed and (b–g) deformed zebrafish: (a) the normal development of (i) finfold, (ii) tail/spinal cord, (iii) cardiac, (iii–iv) yolk sac, cardiac, head and eye; and (b–g) deformed zebrafish: (b) finfold abnormality; (c) tail and spinal cord flexure and truncation; (d) cardiac malformation; (e) yolk sac edema; (f) head edema: (i) head edema; (ii) head edema and eye abnormality; (g) eye abnormality: (i) eye abnormality; (ii) eyeless. Scale bar = 500 Km. Reprinted with permission from ref. 282. Copyright © 2007 American Chemical Society.

**Table 1**

Examples of Plants used to synthesis metal nanoparticles. Adapted from ref. 97

Plant Origin	Metal	Size (nm)
<i>Acalypha indica</i>	Silver	20–30
Apiin extracted from henna leaves	Silver & Gold	39; 7.5–65 (respectively)
<i>Avena sativa</i> (oat)	Gold	5–20 (pH 3–4) & 25–85 (pH 2)
<i>Brassica juncea</i> (mustard)	Silver	2–35
<i>Camellia sinensis</i> (green tea)	Gold	40
<i>Carica papaya</i>	Silver	60–80
<i>Citrus limon</i> (lemon)	Silver	<50
<i>Cochlospermum gossypium</i>	Silver	3
<i>Coriandrum sativum</i>	Gold	6.75–57.91
<i>Cymbopogon flexuosus</i> (lemongrass)	Gold	200–500
<i>Cycas sp.</i> (cycas)	Silver	2–6
<i>Datura metel</i>	Silver	16–40
<i>Desmodium triflorum</i>	Silver	5–20
<i>Eclipta sp.</i>	Silver	2–6
<i>Enhydra fluctuans</i>	Silver	100–400
<i>Eucalyptus camaldulensis</i> (river red gum)	Gold	1.25–17.5
<i>Eucalyptus citriodora</i> (neelagiri)	Silver	~20
<i>Eucalyptus hybrida</i> (safeda)	Silver	50–150
<i>Euphorbia hirta</i>	Silver	40–50
<i>Ficus bengalensis</i> (marri)	Silver	~20
<i>Garcinia mangostana</i> (mangosteen)	Silver	35
<i>Gliricidia sepium</i>	Silver	10–50
Honey	Silver	4
<i>Ipomoea aquatic</i>	Silver	100–400
<i>Jatropha curcas</i> (seed extract)	Silver	15–50
<i>Ludwigia adscendeous</i> (ludwigia)	Silver	100–400
<i>Mentha piperita</i> (peppermint)	Silver & Gold	5–30, 90; 150
<i>Moringa oleifera</i>	Silver	57
<i>Murraya koenigii</i>	Silver & Gold	10; 20
<i>Nelumbo nucifera</i> (lotus)	Silver	25–80
<i>Ocimum sanctum</i> (tulsi; root extract)	Silver	10; 5
<i>Ocimum sanctum</i> (tulsi; leaf extract)	Silver	10–20
<i>Psidium guajava</i> (guava)	Gold	25–30
<i>Scutellaria barbata</i> D. Don (Barbated skullcup)	Gold	5–30
<i>Sesbania drummondii</i> (leguminous)	Gold	6–20
<i>Syzygium aromaticum</i> (clove)	Gold	5–100
<i>Syzygium cumini</i> (jambul)	Silver	29–92

Plant Origin	Metal	Size (nm)
<i>Terminalia catappa</i> (almond)	Gold	10–35

Table 2

A summary of *in vivo* toxicology profiles of nanoparticles. Adapted from ref. 249 and 311

NP	Size	Animal	Mode	Dose	Period	Side effects
AgNP	18 nm	rat	Inhalation	1.73×10 <sup>4</sup> /cm <sup>3</sup> 1.27×10 <sup>5</sup> /cm <sup>3</sup> 1.32×10 <sup>6</sup> particles/cm <sup>3</sup>	6h/day, 5days/week for 4 weeks	Not much notable changes in blood profiles of the both male and female rats
AgNP	18 nm	rat	Inhalation	1.73×10 <sup>4</sup> /cm <sup>3</sup> 1.27×10 <sup>5</sup> /cm <sup>3</sup> 1.32×10 <sup>6</sup> particles/cm <sup>3</sup>	6h/day, 5days/week/12 weeks	Reduced alveolar inflammation & bile duct hyperplasia & liver inflammation
AgNP	18nm	rat	Ingested	30mg/kg, 300 mg/kg and 1000mg/kg	AgNP mixed with diet for 28 days	Changes in alkaline phosphatase activity, cholesterol changes & liver damage
AgNP	13–15	rat	Inhalation	1.73×10 <sup>7</sup> /cm <sup>3</sup> , 0.5 μg/m <sup>3</sup> 1.27×10 <sup>5</sup> /cm <sup>3</sup> 3.5 μg/m <sup>3</sup> 1.32×10 <sup>6</sup> particles/cm <sup>3</sup> 61 μg/m <sup>3</sup>	6h/day, 5days/week/4 weeks	Number of goblet containing neutral mucins in liver increased
AgNP	22 nm	mice	Inhalation	1.97×10 <sup>7</sup> particles/cm <sup>3</sup>	6h/day, 5days/week/2 weeks	Several gene expression related to motor neuronal disorders, neurodegeneration
AuNP	4,10,28,58 nm	Mice	Oral	20,000 μg/kg	7 days	None Observed
AuNP	10, 50 100 and 250 nm	Mice	Tail vein	77–120 μg/kg	24 hr	No adverse effects were noted
AuNP	3.5, 8, 121 7, 37 50	Mice	IP	8,000 μg/kg	21 days	8 – 37 nm AuNP induced severe sickness
AuNP	20 nm	Mice	IV	10 μg/kg	1days 1 week, 1 & 2 months	None noted
AuNP	12.5 nm	Mice	IP	40–400 μg/kg/day	8 days	None noted
AuNP	13.5 nm	Mice (pregnant)	IV, oral, IP	137.5–2200 μg/kg	14 & 28 days	No gold found in the fetuses'